Heliyon 10 (2024) e24050

Contents lists available at ScienceDirect

Heliyon

journal homepage: www.cell.com/heliyon

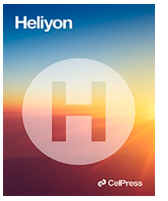

Research article

# Icariin prevents methylmercury-induced experimental neurotoxicity: Evidence from cerebrospinal fluid, blood plasma, brain samples, and in-silico investigations

Sarthak Sharma [a], Sidharth Mehan [a,*], Zuber Khan [a], Ghanshyam Das Gupta [b], Acharan S. Narula [c]

[a] *Division of Neuroscience, Department of Pharmacology, ISF College of Pharmacy (Affiliated to IK Gujral Punjab Technical University, Jalandhar, Punjab, 144603, India), Moga, Punjab, India*
[b] *Department of Pharmaceutics, ISF College of Pharmacy (Affiliated to IK Gujral Punjab Technical University, Jalandhar, Punjab, 144603, India), Moga, Punjab, India*
[c] *Narula Research, LLC, 107 Boulder Bluff, Chapel Hill, NC 27516, USA*

ARTICLE INFO

*Keywords:*
ALS
Methylmercury
Demyelination
Icariin
Oligodendrocytes
Neuroinflammation
Neuroprotection

ABSTRACT

Amyotrophic Lateral Sclerosis (ALS) is a fatal neurodegenerative disease that causes significant neurodegeneration. Methylmercury (MeHg+) is a neurotoxin that induces axonal neurodegeneration and motor nerve degeneration by destroying oligodendrocytes, degenerating white matter, inducing apoptosis, excitotoxicity, and reducing myelin basic protein (MBP). This study examines the inhibition of SIRT-1 (silence information regulator 1), Nrf-2 (nuclear factor E2-related factor 2), HO-1 (heme oxygenase 1), and TDP-43 (TAR-DNA-binding protein 43) accumulation in the context of ALS, as well as the modulation of these proteins by icariin (15 and 30 mg/kg, orally), a glycoside flavonoid with neuroprotective properties. Neuroprotective icariin activates SIRT-1, Nrf-2, and HO-1, mitigating inflammation and neuronal injury in neurodegenerative disorders. In-vivo and in-silico testing of experimental ALS models confirmed icariin efficacy in modulating these cellular targets. The addition of sirtinol 10 mg/kg, an inhibitor of SIRT-1, helps determine the effectiveness of icariin. In this study, we also examined neurobehavioral, neurochemical, histopathological, and LFB (Luxol fast blue) markers in various biological samples, including Cerebrospinal fluid (CSF), blood plasma, and brain homogenates (Cerebral Cortex, Hippocampus, Striatum, mid-brain, and Cerebellum). These results demonstrate that the administration of icariin ameliorates experimental ALS and that the mechanism underlying these benefits is likely related to regulating the SIRT-1, Nrf-2, and HO-1 signaling pathways.

## 1. Introduction

Amyotrophic lateral sclerosis (ALS) is a fatal neurological disorder marked by the gradual breakdown of motor neurons, affecting various brain regions like the cerebral cortex, brain stem, and corticospinal tract [1,2]. In ALS, motor neurons show abnormal TDP-43 aggregates, impairing their nuclear function. Patients experience muscle weakness, respiratory issues, and bulbar region symptoms

* Corresponding author. Division of Neuroscience, Department of Pharmacology, ISF College of Pharmacy (An Autonomous College), NAAC Accredited "A" Grade College, GT Road, Ghal-Kalan, Moga – 142 001 Punjab, India.
*E-mail addresses:* sidharthmehan@isfcp.org, sidh.mehan@gmail.com (S. Mehan).

https://doi.org/10.1016/j.heliyon.2024.e24050
Received 13 October 2023; Received in revised form 29 November 2023; Accepted 2 January 2024
Available online 6 January 2024
2405-8440/© 2024 The Author(s). Published by Elsevier Ltd. This is an open access article under the CC BY-NC-ND license (http://creativecommons.org/licenses/by-nc-nd/4.0/).

like dysarthria and dysphagia. Research indicates a 5 % prevalence rate of ALS in the Indian population [3–5]. Individuals 50 years of age or older have a higher propensity to encounter oxidative stress due to the natural aging process. ALS is only treatable with FDA-approved medications for symptom relief. The following proteins are being investigated as potential selective markers for nutraceuticals targeting MeHg+-induced experimental ALS in rats. We measured their levels to ascertain how icariin affects the neuronal cell proteins SIRT-1, Nrf-2, and HO-1 [6,7].

MeHg+ is a neurotoxic substance that elicits axonal neurodegeneration and motor nerve degeneration by destroying oligodendrocytes, degeneration of white matter, induction of apoptosis, excitotoxicity, and reduction of MBP levels. Furthermore, our initial investigation examines the impact of MeHg+-induced motor neuron death in animal models of ALS progression [1,4,5,8,9]. SIRT-1 is present in brain regions responsible for locomotion, habit formation, and goal-setting [10]. It regulates learning, memory, neurogenesis, inflammation, and ageing. Multiple studies have shown that inhibiting SIRT-1 affects neural plasticity, gene expression, mitochondrial dysfunction, and inflammation [11,12]. Decreased SIRT-1 function and associated causes are responsible for Alzheimer's disease (AD) [13], schizophrenia [14], Parkinson's disease (PD) [14,15], and multiple sclerosis (MS) [16,17]. Consequently, SIRT-1 downregulation in specific brain regions can result in ALS-like symptoms.

Nrf-2 is a key transcription factor managing cellular redox balance and antioxidant response, regulating enzymes like Superoxide dismutase (SOD) and Glutathione peroxidase (GPx). It activates mechanisms to protect cells from oxidative damage by interacting with antioxidant or electrophilic response elements (AREs or EpREs) [18–20]. When the Nrf-2/HO-1 signaling pathway is impaired, cells exhibit increased vulnerability to the adverse effects of PD [21,22], AD [23], MS [24], and depression [25,26]. Reduced Nrf-2/HO-1 signaling levels have been associated with cellular death, disrupted energy metabolism, and impaired mitochondrial function [27]. Hence, the perturbation of the Nrf-2/HO-1 pathway, which has been implicated in the pathogenesis of multiple neurological illnesses leading to aberrations in brain function and neural connectivity, may potentially contribute to the onset and advancement of ALS [28]. Researchers found that Nrf-2/HO-1 controls SIRT-1, revealing interconnectivity between the SIRT-1 and Nrf-2/HO-1 pathways [29, 30]. Enhancing this signaling may prevent neurological dysfunctions, prompting further investigation into their role in ALS. Nutraceuticals, foods, or dietary components with health advantages may aid brain health and treat certain diseases. Icariin is a glycoside flavonoid in plants such as Epimedium [7]. It is well-known for its numerous health benefits [31,32]. Icariin inhibits PDE5, which is responsible for the degradation of cGMP [33]. Free radicals are neutralized by the antioxidant icariin [34]. Free radicals are responsible for cell damage, illness, and aging [35]. Icariin is anti-inflammatory and antioxidant due to its ability to scavenge free radicals. Icariin may have neuroprotective effects. It may prevent oxidative injury to neurons, reduce brain inflammation, and promote neuroplasticity. These effects may be beneficial for AD, PD [34], MS, Schizophrenia [36], and Ischemic Stroke [37,38]. Due to its neuroprotective, anti-inflammatory, and antioxidant properties, icariin can be utilized as a neuroprotective treatment for ALS.

Icariin shows promise in treating neurological disorders by interacting with SIRT-1, Nrf-2, and HO-1. It activates SIRT-1 to reduce beta-amyloid and plaque formation, potentially improving memory, and triggers Nrf-2 and HO-1 to alleviate oxidative stress [39]. Icariin stimulates SIRT-1 to protect dopaminergic neurons from oxidative stress and apoptosis, thereby reducing the development of Parkinson's disease.

Icariin activation of the Nrf-2 pathway and production of HO-1 increases cellular antioxidants and decreases PD-related inflammation [22]. The activation of SIRT-1 by icariin has been observed to protect Huntington's disease (HD) neurons [40]. Icariin has been found to enhance the activity of SIRT-1, leading to improvements in cellular energy utilization and maintenance of protein homeostasis in individuals with HD. Icariin has been observed to stimulate the activation of Nrf-2 and HO-1, exerting a preventive effect against the progression of HD and mitigating oxidative stress [41]. The associations between icariin and the SIRT-1, Nrf-2, and HO-1 pathways suggest it could treat ALS [42]. SIRT-1 activation, crucial in combating ALS, enhances cell survival and mitochondrial function, with Icariin potentially improving neuronal health in ALS by stimulating SIRT-1 [43]. Additionally, Icariin activates the Nrf-2 pathway, increasing antioxidant defense, and stimulating HO-1 expression, highlighting its antioxidant and anti-inflammatory properties. After confirming icariin's effectiveness in vivo, we explored its interaction with SIRT-1, Nrf-2, and HO-1, using both in silico and in vitro methods for validation. Sirtinol, a pharmacological inhibitor [44], targets SIRT-1 and SIRT-2 by binding to their catalytic domains, influencing various cellular pathways. Our study measured SIRT-1, Nrf-2, HO-1, and TDP-43 levels in brain, blood, and CSF samples in ALS, supplemented by behavioral analyses. We also assessed neurochemical, neurobehavioral, and biochemical parameters in various brain regions, using sirtinol to test icariin's efficacy.

## 2. Materials and methods

### 2.1. Animals

In our research, Wistar rats (260–300 gm of body weight; n = 64; equal numbers of either sex) were used, supplied by the Indo-Soviet Friendship College of Pharmacy's internal Animal House in Moga, Punjab, India. All animals were housed at a controlled temperature (25 ± 2 °C) and a 12-h light/12-h Dark cycle (09:00 a.m. - 6:00 p.m.). They were given full access to both food and water. The research design followed the institutional norms for animal care and its use. Efforts were made to reduce the animal's number and any distress. All behavioral tests were conducted in a noise-proof laboratory.

*Ethical approval*

According to Indian law, IAEC (the Institute for Animal Ethics Committee) of the Indo-soviet Friendship College of Pharmacy in Moga, Punjab, India, approved Protocol No. 26 for Project 816/PO/ReBiBt/S/04/CPCSEA at Meeting No. 02/2022. ARRIVE standards were followed while reporting the study. The rats were used in laboratory situations before the investigation phase.

### 2.2. Chemicals and drugs

Sigma–Aldrich supplied the Methylmercury (MeHg+) (St. Louis, MI, USA). The protocol drug icariin was received from RTI International's Drugs Discovery and Development Centre in North Carolina, USA. Antagonist Sirtinol was purchased from Allianz Bio-Innovation. The chemicals used in the study were all of analytical quality. The drugs and chemical solutions were newly made before use. Oral administration of icariin in the form of an aqueous suspension containing 5 % CMC was administered [45].

### 2.3. Animal protocol schedule

Fig. 1 represents the experimental design. From start to finish, the research has taken 42 days. From the 1st to the 21st day, MeHg+ (Toxin) 5 mg/kg was ingested orally (Alam et al., 2022). Icariin has been administered continuously from the 22nd day till the completion of the protocol schedule. Various behavioral assessments were conducted from the 1st to the 42$^{nd}$day (Alam et al., 2022). Each of the 64 animals was assigned randomly to all eight groups. (Group 1st) normal control, (Group 2nd) vehicle control (5 % Carboxymethyl Cellulose from 22 to 42 days), (Group 3rd) icariin 30 mg/kg perse (from 22 to 42 days), (Group 4th) MeHg+ 5 (from 1 to 21 days), (Group 5th) MeHg+ 5 (from 1 to 21 days) + icariin 15 mg/kg (from 22 to 42 days), (Group 6th) MeHg+ 5 (from 1 to 21 days) + icariin 30 mg/kg (5 % CMC from 22 to 42 days), (Group 7th) MeHg+ 5 (from 1 to 21 days) + Sirtinol 10 mg/kg (Antagonist) (from 22 to 42 days) and (Group 8th) MeHg+ 5 (from 1 to 21 days) + icariin 30 mg/kg (from 22 to 42 days) + Sirtinol 10 mg/kg (from 22 to 42 days). On designated days, behavioral tests such as the Grip Strength Test (GST), Open field test (OFT), Forced swim test (FST), as well as the Morris water maze (MWM) were conducted. On day 43, animals were biochemically, inflammatorily, and neurochemically analyzed after being i. p. injected with sodium pentobarbital (270 mg per milliliter) and diffused with chilled Phosphate-buffered saline (0.1 M).

### 2.4. MeHg+ exposure protocol/model of ALS

Our preliminary laboratory results suggest that we have effectively studied and verified rodent models that produce neurobehavioral and neurochemical abnormalities in Wistar rats similar to those in patients with ALS [8,31]. For 21 days, rats were given MeHg+ 5 orally via gavage. According to our preliminary findings, MeHg+ 5, a lethal neurotoxin chemical that can permeate BBB, was found to be identical to ALS's symptoms and neurochemical changes. MeHg+ 5 was, therefore, employed in this study to assess rats' behavioral and neurochemical abnormalities [4,9].

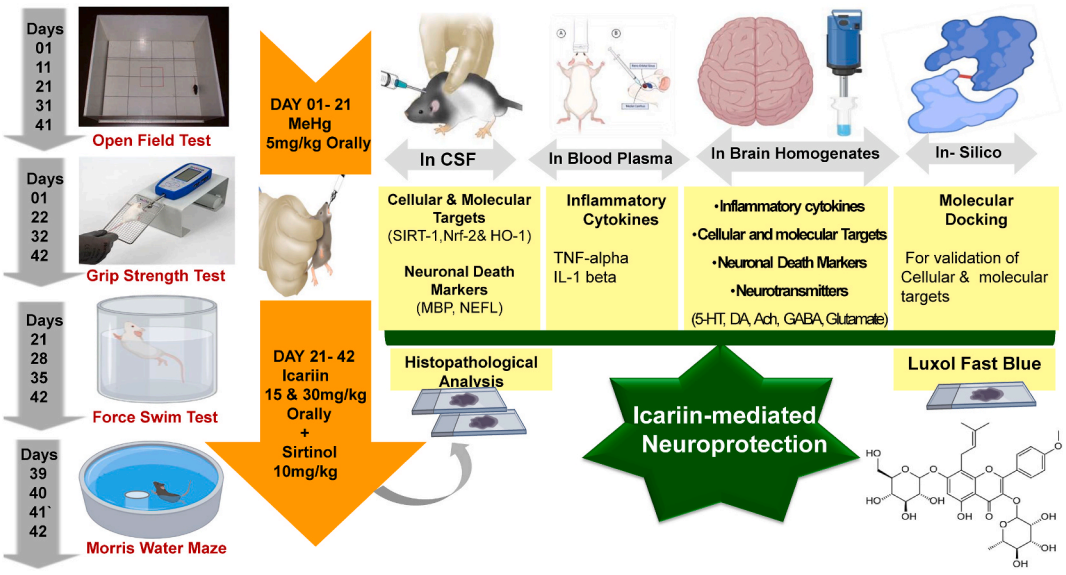


**Fig. 1.** Represents experimental animal design.

### 2.5. Evaluated parameters

#### 2.5.1. Behavioral tests

*2.5.1.1. Open field Task.* An open-field instrument was deployed to observe exploratory movements and nervous behavior. Once the equipment was ready, individually put the rat in the centre of the arena (70 cm × 70 cm) surrounded by white 60 cm walls; the clock was started, & exploratory behavior was permitted for 05 min. Complete quietness was ensured throughout the test session. During the 5-min evaluation, the rodent was allowed to explore its surroundings freely, with a camera capturing its behavior in detail. After each session, the open field where the rodent roamed was meticulously cleaned using soap and water to remove any lingering odours. By analyzing the recorded activity, we determined the frequency and duration of stops at specific locations within the arena, considering the terms "visit" and "stop" as synonymous. Between each rat, the field was appropriately cleaned with 10 % ethanol. The respective rats were returned to their cages after the test was done. The locomotor activity criterion counted the number of rats crossing lines (four paws crossed) and rearing for 5 min. The field trial was conducted on days 1, 11, 21, and 41 [8].

*2.5.1.2. Grip Strength Test.* Musculoskeletal strength, defined as greater endurance of muscles in the front limbs and hindlimbs, is investigated using the rat grip. The test provides valuable information about the overall neuromuscular function and can indicate muscle strength, motor coordination, and endurance changes. The assembly consists of a metal bar attached to a force detector. The rats were examined by grasping a grid connected to a sensor. Rats are retained on the tail and marked as Kilogram-force (Kgf) before holding a grip on both sides. The rats were gently driven back till they let go of the bar. The research timeline measured the gripping potential on days 1st, 22nd, 32nd, and 42nd [9].

*2.5.1.3. Forced swim test.* The Force Swim Test investigates depressive and despair behaviors in rodents by examining their vulnerability to sudden water stress. Rats were placed in a water-filled container and confined in a tank filled with lukewarm water. They were exposed to the tank for 15 min and then refilled. The rats' activities were recorded using a video camera, and immobility time was calculated by keeping their head above water with slight movements [46].

*2.5.1.4. Morris water maze.* The Morris Water Maze test was used to examine rats' spatial memory and recall learning. The rats were placed in a circular tank with 40 cm of water and an escape platform. They were given 120 s to swim freely without an elevated surface before training. After four days, the rats were placed on the platform for 20 s before moving on to the next test. The platform was removed 24 h later for a probing test, determining the extent of cognition consolidation after learning [47].

#### 2.5.2. Evaluation of weight alteration

*2.5.2.1. Evaluation of the body's weight.* The body weight of rats was assessed by a standard digital balance on the days 1st, 7th, 14th, 21st, 28th, 35th, and 42nd. The rats were generally weighed between 10:30 a.m. and 2:00 p.m. to eliminate diurnal variations. This meticulous scheduling ensures a standardized approach to the measurement process, enhancing the accuracy and reliability of the collected body weight data throughout the investigation [48].

*2.5.2.2. Brain-body weight ratio assessment.* The brain/body weight ratios were evaluated at the end of the study to assess the relationship between brain and body weight. A small incision was made behind the occipital bone, and their heads were removed from the rest of their body. The brain was segregated from the spinal cord via the foramen magnum. The rats' skulls were completely detached, and the brains were isolated similarly; the fresh brains were weighed without an olfactory bulb. This methodological approach assesses the proportional relationship between brain mass and overall body weight in the experimental rats [49].

#### 2.5.3. Neurochemical tests

*2.5.3.1. Isolation, preparation, and storage of samples and tissues.* CSF was collected from the rats on day 43 of the experimental schedule, just before the animals were sacrificed. Before beginning, a 26G insulin syringe needle was removed and held by metal forceps at the tip at about 4–5 mm, bending it to a 90°–120° angle. The animal's body was then placed on the customized table and anaesthetized with ketamine at 75 mg/kg. Disconnect the infusion needle from the intravenous infusion set while keeping the lure connector. Attach the 26G insulin syringe needle to the thin tubing. Attach a 1 ml syringe without a needle to a portable holder. Connect the syringe to the tubing that contains a bent needle.

Anaesthetizing the animal at a 75 mg/kg dose with ketamine is the initial step in collecting CSF. After that, we shaved the rats' heads and disinfected them with ethanol (at 75 %). The anaesthetized rat's body is placed on the customized table, and the animal's head is positioned above the opening and attached to the rodent ventilator. Optic infections can be treated with erythromycin eye ointment. The foramen magnum can be easily seen when the rat is placed vertically, head down. After the foramen magnum has been located, gently hold the rat's head in one hand to prevent unnecessary stress and harm, and insert the bent needle vertically into the skin behind the foramen magnum with the other. After transferring CSF to a microcentrifuge tube with an insulin syringe, the sample should be centrifuged for 10 min at 10,000×*g* for 5 min at 40C.

On the same day, 43rd, 2.5 ml of blood was taken by piercing the Retro orbital plexus and putting the capillary tube in the eye of the rat. Blood was extracted from the nerve plexus using capillary action by continuously rotating and pulling the tube into an Eppendorf tube containing purified and sterile EDTA [5]. Freshly taken blood was centrifuged at 10,000 rpm for 15 min to separate the plasma from the remaining fluid of the blood. The plasma was subsequently preserved in a deep freezer at −80 C for later use.

After the collection of blood and CSF, the rats were beheaded. Brains were isolated and stored in ice-cold PBS (0.1 M) before being analyzed biochemically in PBS. The blood's plasma was isolated from freshly obtained blood by centrifugation at 10,000 g for 15 min, and the supernatant was stored for later use (at −80 C) in a deep refrigerator [5]. Each fresh brain weight was measured before gross pathology, brain sectioning, histopathology, and the LFB approach. They were made homogeneous after mixing the brain samples with a 3–4 chilled homogenate liquid per tissue volume. Using a mechanical shear homogenizer, the tissue was homogenized 3–4 times for 20–30 s each time, with a 10–15-s pause. The homogenate was centrifuged at 10,000 g for 10–20 min at 4 °C to remove cellular debris and other particulates, and it was refrigerated at −80 °C till other tests [9,49].

Each fresh brain was measured before the gross pathology, brain sectioning, histopathology, and LFB approach. After the brain samples were mixed with a 3–4 volume chilled homogenate liquid per tissue volume, they were made homogeneous [50].

Gross pathological examination with neurological degeneration volume in coronal, midbrain, and cerebellum regions.

Rats were sacrificed on day 43, and their brains were separated for gross pathological analysis. Following an examination of the entire rat brain, coronal slices were arranged. Brain tissue sections 2 mm thick were obtained and displayed on glass slides. All brains were captured using a digital camera (Fujix digital camera, Fujifilm, Japan). During the 43rd day of the process, the demyelinated region (mm3) of each brain section was measured with the MOTICAM-BA310 image plus 2.0 analytical programmers. The demyelination volume was estimated by transforming the area for every coronal brain, midbrain (mm3), and cerebellum section into a volume (mm3). An imaging scan was carried out on the 43rd day to detect the level of degeneration (mm3) in each brain region [46].

### *2.5.4. ELISA assay kits*

Following ELISA Kits were used to measure cellular and molecular targets, ELISA kits [E-EL-R1102, Elabsciences, Wuhan, China] were applied to measure SIRT-1 protein levels [9,16]. Nrf-2 in the rat brain tissue and CSF samples were measured using an ELISA kit [E2639Ra, BT Lab, Shanghai, China] [1]. HO-1 in rat brain tissue and CSF was estimated using ELISA assay kits from [E-EL-R2110, Elabscience, Wuhan, China]. The testing kit for the TDP-43 ELISA Kit was obtained from [KBH6246, KRISHGEN, Maharashtra, India] [16]. TNF-α levels in homogenates of rat brain & blood plasma through a diagnostic kit [KB1145, KRISHGEN, Maharashtra, India] (Khera et al., 2017). IL-1beta level in rat brain homogenate was measured using a diagnostic kit [KLR0119, KRISHGEN, Maharashtra, India] [9]. An ELISA kit [KLR1648, KRISHGEN, Maharashtra, India] was used to measure the quantity of Caspase-3 in brain tissue and blood plasma. Bax [KLR0034, KRISHGEN, Maharashtra, India] [8]. Bcl-2 levels were measured using an ELISA kit [KLR0034, KRISHGEN, Maharashtra, India] [16]. ELISA test kits measured the MBP level in the brain homogenate of rats and cerebral spinal fluid [E-EL-R2536, Elabscience, Wuhan, China] [51]. The total concentration of acetylcholine was measured using an ELISA kit [KLR0722, KRISHGEN, Maharashtra, India] [52]. Dopamine levels were measured using the ELISA kit [KLR0219, KRISHGEN, Maharashtra, India] [9]. GABA level was measured using an ELISA Kit [KLR0102, KRISHGEN, Maharashtra, India] [5]. Glutamate level was measured using an ELISA Kit [KLR1474, KRISHGEN, Maharashtra, India]. Serotonin levelss were measured using an ELISA Kit [KLR0866, KRISHGEN, Maharashtra, India] [9].

### *2.5.5. Quantification of MeHg+*

The high selectivity fluorescence assay provided by the Mercury Assay Kit (ab233467) allows for the precise measurement of mercury ion (MeHg+). The brain was homogenized in purified water (Kinematica GmbH, Littau, Switzerland) using a Polytron homogenizer (10 %, w/v). Add 25 μL of DMSO into the vial of Mercury sensor 590 to make 200× stock solution. To prepare the mercury analysis mixture, combine 25 μL of Mercury sensor 590 stock solution with 5 mL of Assay Buffer. As for the mercury (II) standard, we used Mercury (II) Perchlorate hydrate (CAS#304656-34-6). Mercury (II) stock solution was made with a concentration of 1 mM in ddH2O. The stock solution should be separated for individual use and kept at – 20 °C. To a 96-well black microplate, add 50 μL serial dilutions of a mercury (II) standard and MeHg+-containing samples for testing. Put 50 μL of blank Assay Buffer into each well of a 96-well black microplate. To make a total volume of 100 μL/well, add 50 μL of mercury assay mixture to each well containing a mercury (II) standard, blank control, and test sample. Then, we incubated out of the light at room temperature for 20–30 min. The plate reader fluorescence is then measured at Ex/Em = 540/590 nm, cutoff 570 nm. The level was expressed as μg/g [53].

### *2.5.6. Histopathological examination*

Sodium Phenobarbital was used to induce unconsciousness in rats, and their brains were separated for histological analysis. Coronal sections, midbrain, and cerebellum were separated from other brain regions. The sections were preserved in 4 % paraformaldehyde and coated in paraffin. The morphology was examined using a fluorescence microscope, revealing healthy neurons in the cerebellar cortex, hippocampus, and cerebellum region [9]. Luxol Fast Blue (LFB) Examination.

The same technique was used for histopathology once the rat's cerebral cortex was mounted on slides. The slides containing rat brain tissue were deparaffinized in xylene for 30 min thrice. Five minutes of clearing with 100 % alcohol were followed by three passes with 95 % alcohol to remove all traces of xylene. The slides were then placed in a Petri dish containing a 5 % Luxol Fast Blue solution and incubated at 50 °C for 12 h. After a minute at room temperature, the slides were cleaned in 95 % ethanol. They were carefully rinsing the slide under running water. Separation was achieved by adding 0.05 % lithium carbonate to the Petri dish for 5–20 s. The slide went unnoticed until its grey matter lost its coloration. The slide was washed with 70 % ethanol thrice, once for 1 min and once for ten. The slides were looked at with a Nikon Type 102 M fluorescence microscope with a 40× magnification.

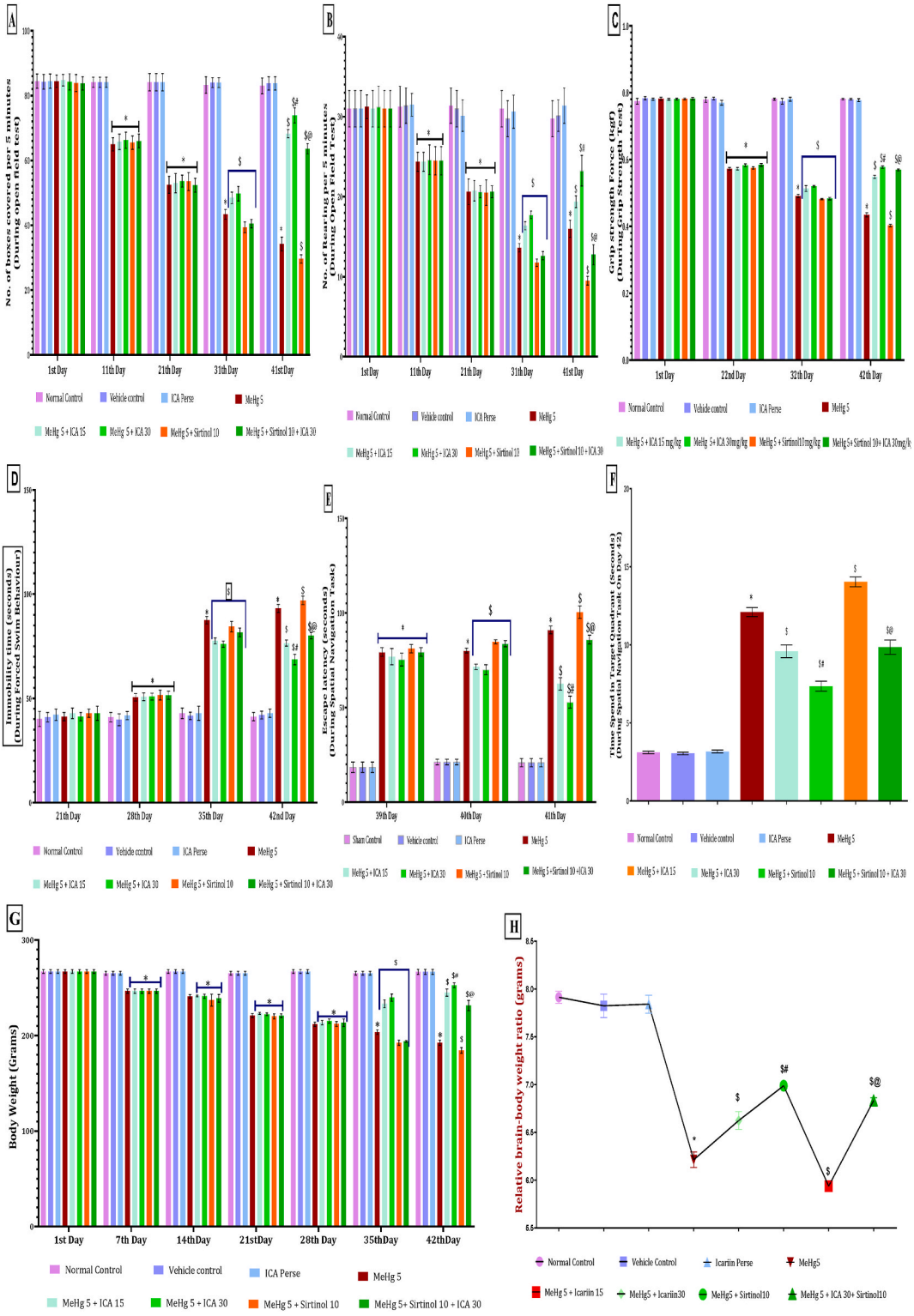


**Fig. 2.** (A–H). Icariin-mediated neuroprotective potential improves and restores locomotion activity [2A]; rearing behavior [2B]; muscle grip strength [2C]; Immobility time [2D]; escape latency time [2E]; TSTQ [2F]; body weight [2G] and relative brain-body ratio [2H] in experimental ALS rats. *The statistical data analysis presented by two-way analysis of variance (ANOVA) with post-hoc test Bonferroni's. Values presented as mean ± S. D [n = 8 wistar rats in each experimental group; p < 0.01].* *Versus Normal-control, Vehicle control and icariin perse control; **$** Versus MeHg 5, **$#** Versus icariin 15; and **$@** Versus MeHg5, Sirtinol 10, icariin 30* (Fig. 2A, B, 2C, 2D, 2E, 2G).

#### 2.5.7. Molecular docking

Molecular docking can help identify and predict the binding sites on the receptor where ligands interact to induce activation [33]. By simulating the docking process, it can explore different regions of the receptor and determine the most probable binding sites for ligand binding and subsequent activation, and allow investigation of the specific interactions between ligands and the receptor, such as hydrogen bonding, hydrophobic interactions, and electrostatic interactions [54]. These interactions play a vital role in receptor activation by stabilizing ligand-receptor complexes and transmitting signals within the receptor [55,56]. To find the binding interactions of the protocol drug icariin with our selected targets, HO-1 (PDB ID: 3HOK) crystallographic receptor of human heme oxygenase (https://www.rcsb.org/structure/3HOK) [57]. NRF-2 (PDB ID: 5CGJ) crystal structure of murine Keap1 selective activator of Nrf-2 signaling (https://www.rcsb.org/structure/5CGJ) (Heyninck et al., 2016). SIRT-1 crystallographic receptor of SIRT-1 (PDB ID: 5BTR) (https://www.rcsb.org/structure/5BTR) was used for molecular docking studies [58]. Before molecular docking, the retrieved crystal structure underwent preparation steps that involved the removal of water and ions, as well as the addition of nonpolar hydrogens. The protein was subjected to minimization and optimization using AutoDock Tool v1.5.7 as a preliminary step before initiating the docking process (https://autodocksuite.scripps.edu/adt) [59], bundled with the MGLTools package ver.1.5.6 (https://ccsb.scripps.edu/mgltools) [60]. Energy minimization and conversion to. pdbqt format of protocol drug icariin were carried out in PyRx [61]. The PyRx virtual screening tool was employed to carry out molecular docking (https://sourceforge.net/projects/pyrx) [62]. During the docking process, standard size grids were placed at default docking algorithm positions in the active site pocket of (PDB ID: 3HOK) at coordinates X = 13.30, Y = 25.41, Z = 10.46 (PDB ID: 5CGJ), at coordinates X = 40.01, Y = −10.60, Z = 8.12, and (PDB ID: 5BTR) at coordinates X = −20.16, Y = 66.96, Z = 3.23. To study the interactions between the best poses generated by molecular docking, Discovery Studio version v21.1.0.20298 was employed [63].

#### 2.5.8. Statistical analysis

Using prism software (Graph pad prism 8.0.1, San Diego, CA, USA), the recorded values from various experiments were statistically analyzed. The neurochemical parameters were evaluated by one-way ANOVA with repeated measures and Tukey's post-hoc test for multiple comparisons. In addition, a two-way analysis of variance (ANOVA) followed by post-hoc Boferroni's test was used to assess differences in neurobehavioural evaluation between treatment groups. The experimental data were represented graphically as mean with standard deviation (SD). The significance criterion for results was set at the $p < 0.01$ probability level.

## 3. Results

### 3.1. Icariin-mediated neuroprotective potential on neurobehavioral alteration in experimental ALS rats

#### 3.1.1. Icariin-mediated neuroprotective potential improves locomotion behavior in experimental ALS rats

The study recorded locomotion and rearing of MeHg 5-exposed ALS rodents in an OFT. Compared to rats given icariin or vehicle control, rats treated with MeHg 5 showed decreased locomotion and increased rearing activity. Taking icariin 15 and icariin 30 orally significantly enhanced movement [two-way ANOVA: $F(7,56) = 1425, p < 0.01$] and decreased anxiety [two-way ANOVA:$F(7,56) = 309.0, p < 0.01$] in comparison to the normal, vehicle control, and icariin 30 per se administered groups. The treatment of rodents with Sirtinol 10 alone led to a greater decline in locomotion and anxiety-like behavior compared to MeHg 5, whereas the combination showed a significant increase (Fig. 2A and B).

#### 3.1.2. Icariin-mediated neuroprotective improves muscle grip strength in experimental ALS rats

The study found no significant difference in grip strength between the normal vehicle control group and the icariin 30 perse group, but significantly less grip strength on day 22. Animals administered icariin 15 or icariin 30 on days (32nd to 42nd) demonstrated a dose-dependent and statistically significant increase in muscular grip strength force compared to MeHg 5- treated rats [two-way ANOVA:$F(7,56 = 1378), p < 0.01$]. On day 42, icariin 30 mg/kg-treated rats demonstrated significantly greater muscle grip strength than icariin 15 mg/kg-treated rats. In contrast, the Sirtinol 10- alone-treated group had weaker grasp strength than the icariin 15 mg/kg and icariin 30 mg/kg-treated groups. In addition, compared to the Sirtinol 10 mg/kg group, the icariin 30 mg/kg group demonstrated significant increases in grip strength (Fig. 2C).

#### 3.1.3. Icariin-mediated neuroprotective potential improves immobility time in experimental ALS rats

The Force swim test revealed that Wistar rats exposed to MeHg 5 exhibited depressed behavior and longer periods of immobility compared to the normal control and icariin 30 perse-treated rats. Compared to the MeHg 5 administered group [two-way ANOVA:$F(7,56 = 723.5), p < 0.01$], regular oral administration of icariin 15 and icariin 30 for 21 days significantly reduced the duration of immobility on days 28, 35, and 42. The combination of Sirtinol 10 mg/kg and icariin 30 mg/kg significantly reduces depressive-like behavior by reducing immobility time compared to the Sirtinol 10 mg/kg group (Fig. 2D).

#### 3.1.4. Icariin-mediated neuroprotective potential restores memory and cognitive impairment in experimental ALS rats

The escape latency test was conducted on days 38, 39, 40, and 41 of the protocol schedule. Consistent MeHg 5 dosing over 21 days causes a substantially more significant increase in ELT in ALS rats compared to the normal, vehicle, and icariin 30 perse groups. Chronic treatment with icariin 15 and icariin 30 for the subsequent 21 days decreased ELT in a dose-dependent manner compared to the MeHg 5 treated group [two-way ANOVA:$F(7,56) = 3177, p < 0.01$]. In addition, icariin 30-treated rodents regained their long-term memory more effectively than icariin 15-treated rats. In contrast, Methylmercury treatment of ALS rats significantly increased Escape

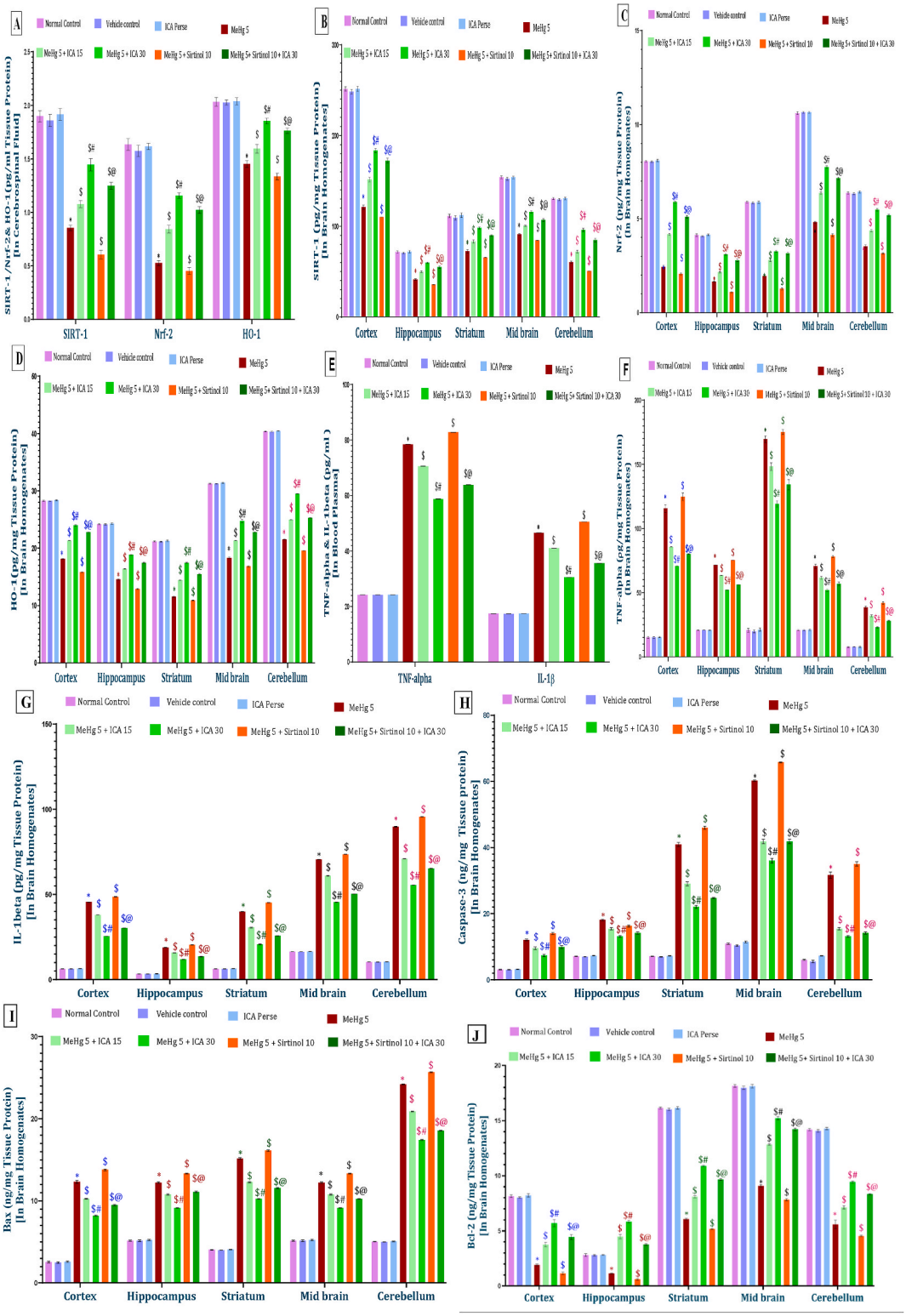


**Fig. 3. (A–J). Icariin-mediated neuroprotective potential modulates SIRT-1, Nrf-2 & OH-1 levels [3A], SIRT-1 [3B], Nrf-2 [3C], & OH-1 [3D] levels, Inflammatory cytokines TNF-α & IL-1β levels [3E], TNF-α level [3F], IL-1β level [3G], caspase-3 level [3H], Bax level [3I], and Bcl-2 levels [3J] in experimental ALS rats.** *The statistical data analysis was presented using one-way ANOVA analysis using the Tuckeys test. Values presented as mean ± S. D [n = 8 wistar rats in each experimental group; p < 0.01]. *Versus Normal control, Vehicle control, and icariin perse control; $ Versus MeHg 5; $# versus icariin 15; and $@ Versus MeHg 5, Sirtinol 10, icariin 30* [Fig. 3A, B, 3C, 3D, 3E, 3F, 3G, 3H, 3I, 3J].

Latency Time, whereas Sirtinol 10 alone had no effect. When combined with Sirtinol 10 and icariin 30, the escape latency time of ALS rats is significantly reduced (Fig. 2E).

On day 42 of the protocol, each group's duration in the TSTQ was measured. Compared with the control, vehicle, and icariin 30 perse groups, the TSTQ of rats treated with MeHg 5 decreased progressively. Icariin 15 and icariin 30 significantly increased TSTQ compared to MeHg 5- exposed rats [one-way ANOVA:F (7,49 = 0.8572,p < 0.01]. The icariin 30 mg/kg treatment group significantly enhanced long-term memory. In contrast, Sirtinol 10 alone led to a substantial reduction in Time Spent in the Target Quadrant. In addition, the combination of icariin 30 and Sirtinol 10 was more effective than Sirtinol 10 alone (Fig. 2F).

### *3.1.5. Icariin-mediated neuroprotective potential improves body weight variance in experimental ALS rats*

*3.1.5.1. Icariin improves body weight in experimental ALS rats.* Throughout the investigation, the variation in rat body weight was measured weekly. There were no significant differences between the Normal, vehicle, and icariin 30 groups throughout the study. In addition, by the seventh day, the MeHg 5 treated group had significantly less body weight than the control, vehicle, and icariin 30 perse groups. On the 28th day, the icariin and Sirtinol treated groups gained weight. In contrast, prolonged oral administration of icariin 15 and icariin 30 to rats for 21 days resulted in a steady increase in body weight [two-way ANOVA:F (7,56) = 1378),p < 0.01]. The icariin 30 group was significantly more efficacious at increasing body weight than the icariin 15 group. The group treated with Sirtinol 10 alone lost more weight than those treated with icariin 30. Moreover, compared to the Sirtinol 10 alone-administered group, combining icariin 30 and Sirtinol 10 resulted in more remarkable gains in body weight (Fig. 2G).

*3.1.5.2. Icariin improves brain-body weight in experimental ALS rats.* The brain-body weight ratio was measured on day 42 of the experimental protocol. No significant difference existed between the Normal-control, vehicle, and icariin 30 groups. Compared to the normal, vehicle, and icariin 30 perse groups, the relative brain-to-body weight ratio in the MeHg 5 group decreased significantly. Chronic treatment of MeHg 5 exposed ALS rats with icariin 15 and icariin 30 increased the relative brain-body weight ratio [one-way ANOVA:F (7,49) = 2.049,p < 0.01]. When restoring the rat's relative brain-body weight ratio, icariin 30 was more effective than icariin 15. Nevertheless, Sirtinol 10 alone decreases the relative brain-body weight ratio compared to icariin 30. In addition, the ratios in the icariin 30 and Sirtinol 10 groups increased significantly compared to the Sirtinol 10 group (Fig. 2H).

*A one-way ANOVA analysis was done using the Tuckeys test. Values presented as mean ± S. D [n = 8] wistar rats in each experimental group; p < 0.01].*Versus Normal-control, Vehicle control, and icariin perse control;* ***$*** *Versus MeHg 5,* ***$#*** *Versus icariin 15; and* ***$@*** *Versus MeHg5, Sirtinol 10, icariin 30 (2F, 2H).*

### *3.1.6. Icariin-mediated neuroprotective potential on neurochemical alteration in experimental ALS rats*

*3.1.6.1. Icariin-mediated neuroprotective potential modulates SIRT-1, Nrf-2, and HO-1 levels in experimental ALS rats.* Following the completion of the procedure, CSF samples were analyzed for the presence of SIRT-1, Nrf-2, and HO-1. After 21 days of oral administration of MeHg 5, SIRT-1, Nrf-2, and HO-1 concentrations were significantly reduced compared to the Normal, vehicle, and icariin 30 perse groups. One-way analysis of variance (ANOVA) revealed statistically significant differences between cerebrospinal fluid, SIRT-1 (one-way ANOVA:F (7,49) = 1.509,p < 0.01), Nrf-2 (one-way ANOVA:F (7,49) = 0.601,p < 0.01), and HO-1 (one-way ANOVA: F (7,49) = 0.2815,p < 0.01). It has been demonstrated that icariin 30 mg/kg is more productive than icariin 15 mg/kg at restoring SIRT-1, Nrf-2, and HO-1 protein levels in numerous biological samples. Sirtinol 10 mg/kg reduces SIRT-1, Nrf-2, and HO-1 levels significantly. Sirtinol 10 mg/kg was ineffective at restoring SIRT-1, Nrf-2, and HO-1 protein expression in rat CSF, whereas Sirtinol 10 mg/kg in combination with icariin 30 mg/kg was more effective (Fig. 3A).

Upon completion of the procedure, samples of the rat's brain tissue were examined for the presence of SIRT-1. After 21 days of oral administration of MeHg 5 to the Normal, vehicle, and icariin 30 perse groups, SIRT-1 concentrations were significantly reduced. One-way analysis of variance (ANOVA) revealed significant differences between brain homogenate of different brain regions, including SIRT-1 (one-way ANOVA:F (7,49) = 1.499,p < 0.01) in the cortex, SIRT-1 (one-way ANOVA:F (7,49) = 1.772, p < 0.01) in the hippocampus, SIRT-1 (one-way ANOVA:F (7,49) = 0.9804,p < 0.01) in the striatum, (one-way ANOVA:F (7,49) = 4.965,p < 0.01) in Midbrain, (one-way ANOVA:F (7,49) = 1.396,p < 0.01) in Cerebellum. Sirtinol 10 mg/kg reduces SIRT-1 levels significantly. Sirtinol 10 mg/kg was ineffective at restoring SIRT-1 protein expression in rat brains, whereas Sirtinol 10 mg/kg in combination with icariin 30 mg/kg was more effective (Fig. 3B).

Following the procedure, rat brain tissue samples were examined for the presence of Nrf-2. After 21 days of oral administration of MeHg 5, Nrf-2 concentrations were significantly lower than in the Normal, vehicle, and icariin 30 perse groups. Nrf-2 (one-way ANOVA:F (7,49) = 1.417,p < 0.01) in the cortex, Nrf-2 (one-way ANOVA:F (7,49) = 0.653, p < 0.01) in the hippocampus, Nrf-2 (one-way ANOVA:F (7,49) = 0.583,p < 0.01) in the striatum, (one-way ANOVA:F (7,49) = 0.796,p < 0.01) in the midbrain, (one-way ANOVA:F (7,49) = 0.921,p < 0.01) in the cerebellum and Sirtinol 10 mg/kg significantly lowers levels of Nrf-2. Sirtinol 10 mg/kg alone was ineffective in restoring Nrf-2 protein expression in the rat brain, whereas combination treatment with 30 mg/kg of icariin was more efficacious (Fig. 3C).

After the procedure, rat brain tissue samples were examined for the presence of HO-1. After 21 days of oral MeHg 5 administration, HO-1 concentrations were significantly lower than in the Normal, vehicle, and icariin 30 perse groups. Levels of HO-1 (one-way ANOVA:F (7,49) = 1.608,p < 0.01) in the cortex, (one-way ANOVA:F (7,49) = 0.851,p < 0.01) in the hippocampus, (one-way ANOVA: F (7,49) = 1.116,p < 0.01) in the striatum, (HO-1; F (7,49) = 0.788,p < 0.01) in the midbrain, (one-way ANOVA:F (7,49) = 1.016,p <

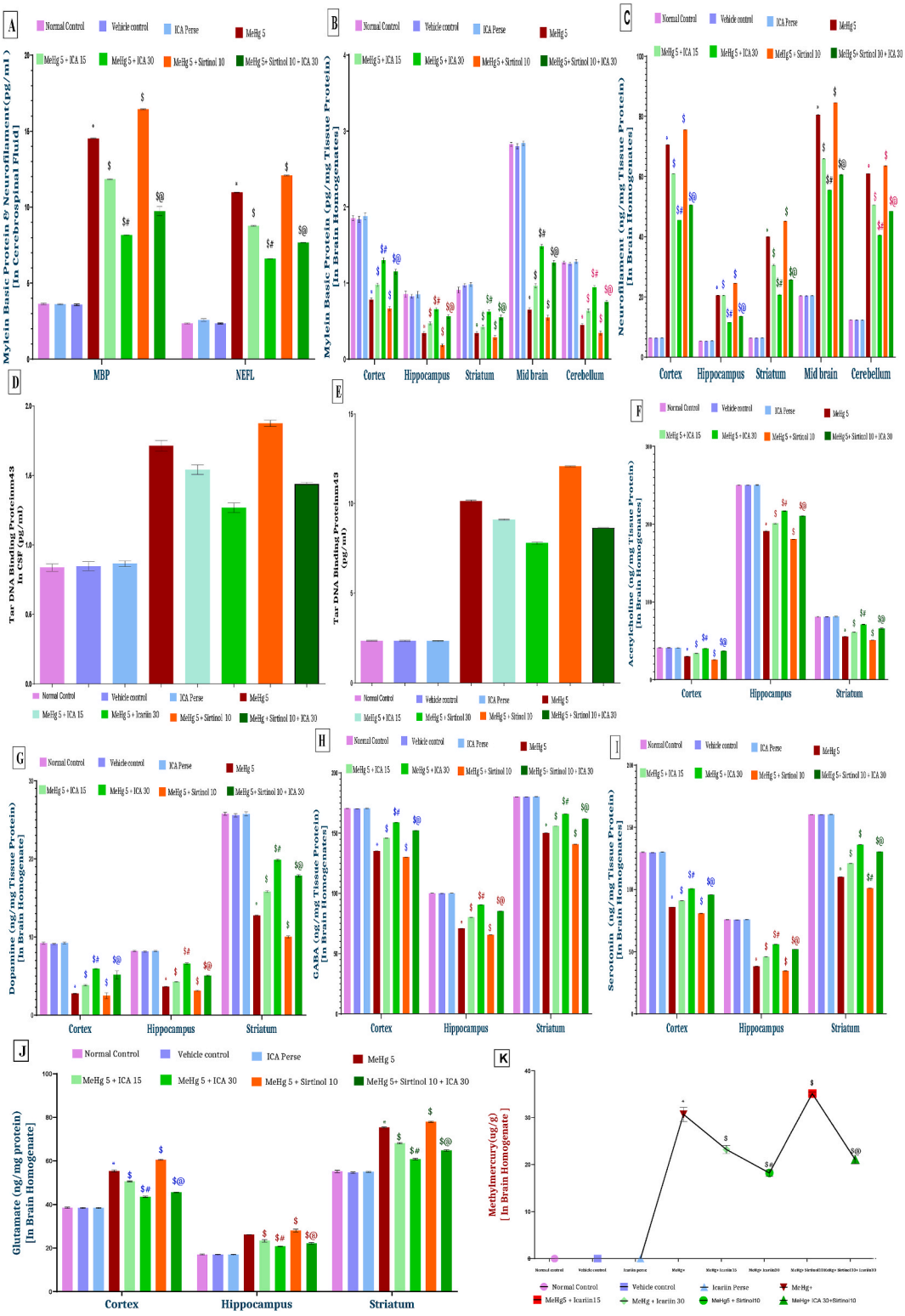


**Fig. 4. (A–K). Icariin-mediated neuroprotective potential modulates NEFL & MBP levels [4A]; MBP levels [4B]; NEFL levels [4C]; TDP43 levels [4D, 4E]; acetylcholine [4F]; Dopamine [4G]; GABA [4H]; Serotonin [4I]; Glutamate [4J] and Methylmercury levels [4K] in experimental ALS rats.** *The statistical data analysis presented using one-way ANOVA analysis by using Tuckeys test. Values presented as mean ± S. D [n = 8 wistar rats in each experimental group; p < 0.01]. *Versus Normal, Vehicle control and icariin perse control; $ Versus MeHg 5; $# versus icariin 15; and $@ Versus MeHg 5, Sirtinol 10, icariin 30 [*Fig. 4A, B, 4C, 4D, 4E, 4F, 4G, 4H, 4I, 4J, 4K*].*

0.01) in the cerebellum. Sirtinol 10 mg/kg significantly reduces HO-1 levels. Sirtinol 10 mg/kg alone was ineffective in restoring HO-1 protein expression in the rat brain, whereas combination treatment with 30 mg/kg of icariin was more efficacious (Fig. 3D).

*3.1.6.2. Icariin-mediated neuroprotective potential decreases inflammatory cytokines levels in experimental ALS rats.* To determine the neuroprotective effect of icariin on pro-inflammatory cytokines, we measure the levels of tumor necrosis factor-alpha (TNF-alpha) and interleukin-1beta (IL-1β) in the blood plasma of rodents. After treatment with icariin 15 and icariin 30, TNF- levels were significantly reduced in blood plasma [One-way ANOVA:F (7,49) = 1.926,p < 0.01]. Both icariin 15 and icariin 30-treated rats had elevated levels of IL-1 in their blood plasma [One-way ANOVA:F (7,49) = 1.027,p < 0.01]. Icariin 15 reduced neuroinflammatory cytokines, while icariin 30 was more effective. Sirtinol 10 treatment significantly reduced TNF-alpha and IL-1beta levels compared to icariin 30 and Sirtinol 10 (Fig. 3 E).

In order to determine the neuroprotective effect of icariin on the pro-inflammatory cytokines, we analyzed the levels of tumor necrosis factor-alpha (TNF-alpha) and interleukin-1 (IL-1beta) in the brain tissues of rats. As a result of treatment with icariin 15 and icariin 30, TNF-alpha levels decreased significantly in Cortex [One-way ANOVA: F (7,49) = 0.889,p < 0.01]; Hippocampus [One-way ANOVA:F (7,49) = 2.915,p < 0.01]; Striatum [One-way ANOVA:F (7,49) = 1.543,p < 0.01]; Mid Brain [One-way ANOVA:F (7,49) = 1.682,p < 0.01]; and Cerebellum [One-way ANOVA: F (7,49) = 2.290,p < 0.01]. Rats given icariin 15 or icariin 30 showed decreased levels of IL-1beta in both the brain tissue Cortex [One-way ANOVA: F (7,49) = 2.940,p < 0.01], in Hippocampus [One-way ANOVA:F (7,49) = 0.2990,p < 0.01], in Striatum [One-way ANOVA:F (7,49) = 0.973,p < 0.01], In Mid Brain [One-way ANOVA: F (7,49) = 0.6442,p < 0.01], and In Cerebellum [One-way ANOVA:F (7,49) = 0.468,p < 0.01]. Icariin 15 effectively reduced the levels of these neuroinflammatory cytokines, but icariin 30 was much more effective. TNF-alpha and IL-1beta levels in brain tissue were also markedly higher in the Sirtinol 10 treatment group compared to the icariin 30 treatment group. In addition, when given together, TNF-alpha and IL-1beta levels were significantly reduced compared to the Sirtinol 10-treated group (Fig. 3F and G).

*3.1.6.3. Icariin-mediated neuroprotective potential modulates bax and Caspase-3 levels in experimental ALS rats.* Caspases-3 and other apoptotic markers were measured in brain tissue following the completion of the procedure. When MeHg 5 was administered orally for an extended period of time, pro-apoptotic markers, such as caspase-3, increased dramatically. Brain tissue homogenates such as Cortex [One-way ANOVA:F (7,49) = 0.857,p < 0.01], Hippocampus [One-way ANOVA:F (7,49) = 0.608,p < 0.01], Striatum [One-way ANOVA:F (7,49) = 0.5353, p < 0.01], Mid brain [One-way ANOVA:F (7,49) = 1.666,p < 0.01], and Cerebellum [One-way ANOVA:F (7,49) = 0.609,p < 0.01], Caspase-3 levels were decreased following long-term administration of 15 mg/kg and 30 mg/kg icariin orally. Sirtinol 10 alone causes a substantial rise in caspase levels in brain homogenates. When Sirtinol 10 and icariin 30 were administered together, the caspase level decreased significantly compared to the sirtinol 10 group.

Following the surgical procedure, apoptotic markers such as Bax were detected in brain tissue. When MeHg 5 was administered orally for an extended period of time, pro-apoptotic markers, such as Bax, increased dramatically. As a result of chronic oral administration of icariin 15 and icariin 30, Bax levels decreased in brain tissue homogenates, such as Cortex [One-way ANOVA:F (7,49) = 2.239,p < 0.01], Hippocampus [One-way ANOVA:F (7,49) = 0.8379,p < 0.01], Striatum [One-way ANOVA:F (7,49) = 0.4141,p < 0.01], Midbrain [One-way ANOVA:F (7,49) = 1.414,p < 0.01], and Cerebellum [One-way ANOVA:F (7,49) = 0.993,p < 0.01]. The Sirtinol 10 group experienced a greater increase in Bax than the icariin 30 group. Bax levels were significantly decreased in the Sirtinol 10 + icariin 30 treatment group compared to the Sirtinol 10 treatment group (Fig. 3H and I).

Moreover, after 21 days of continuous treatment with icariin 15 and icariin 30, the level of Bcl-2 protein in the brain homogenate of MeHg 5- treated rodents was significantly elevated. Brain tissue homogenates including the Cortex (One-way ANOVA: F (7,49) = 1.572,p0.01), Hippocampus (One-way ANOVA: F (7,49) = 0.4546,p < 0.01), Striatum (One-way ANOVA: F (7,49) = 3.948,p < 0.01), Midbrain (One-way ANOVA:F (7,49) = 3.346,p < 0.01), and Cerebellum (One-way ANOVA: F (7,49) = 1.503,p < 0.01] When it came to restoring the level of apoptotic markers, icariin 30 treatment was more efficacious than icariin 15 treatment. The sirtinol 10 treatment led to a more significant reduction in Bcl-2 than the icariin 30 treatment. Furthermore, the Bcl-2 level was substantially higher in the icariin 30-treated group compared to the Sirtinol 10-treated group (Fig. 3J).

*3.1.6.4. Icariin-mediated neuroprotective potential modulates NEFL and MBP levels in experimental ALS rats.* An ELISA kit determined CSF's demyelinating protein MBP and Neurofilament levels. Compared to the control, vehicle, and icariin 30 perse groups, the MeHg 5 treatment significantly increased MBP and NEFL levels. In conclusion, continued administration of icariin 15 and icariin 30 restored MBP levels in CSF [one-way ANOVA:F (7,49) = 1.094,p < 0.01] and NEFL [one-way ANOVA:F (7,49) = 0.733,p < 0.01]. With icariin 30, MBP and NEFL levels were restored substantially more effectively than with icariin 15. In addition, the Sirtinol 10 group experienced a greater increase in MBP and NEFL levels than the icariin 30 group. MBP and levels reduced substantially more when combined with icariin 30 and Sirtinol 10 than when Sirtinol 10 was used alone (Fig. 4A).

*3.1.6.5. Icariin-mediated neuroprotective potential modulates MBP levels in brain homogenates.* An ELISA kit assessed the quantity of demyelinating protein (MBP) in brain homogenate. Compared to the control, vehicle, and icariin 30 perse groups, long-term MeHg 5 treatment significantly decreased MBP levels. In conclusion, continued administration of icariin 15 and icariin 30 resulted in significant restoration of MBP levels in brain homogenate, including Cortex [One-way ANOVA:F (7,49) = 1.084,p < 0.01], Hippocampus [One-way ANOVA:F (7,49) = 4.637,p < 0.01], Striatum [One-way ANOVA:F (7,49) = 1.096,p < 0.01], Midbrain [One-way ANOVA:F (7,49) = 0.222,p < 0.01], Cerebellum [One-way ANOVA:F (7,49) = 1.800,p < 0.01]. Icariin 30 was more effective in restoring MBP than icariin 15, and Sirtinol 10 treatment led to a greater MBP decrease, with MBP levels improving more when combined (Fig. 4B).

Long-term MeHg 5 treatment significantly increased NEFL levels in brain homogenate, while sustained icariin 15 and 30 administration significantly decreased NEFL levels. Icariin 30 decreased NEFL levels substantially more effectively than icariin 15 in brain tissue homogenates, including Cortex [One-way ANOVA:F (7,49) = 1.706,p < 0.01], Hippocampus [One-way ANOVA:F (7,49) = 2.698,p < 0.01], Striatum [One-way ANOVA:F (7,49) = 1.706,p < 0.01], Midbrain [One-way ANOVA:F (7,49) = 1.132,p < 0.01], Cerebellum [One-way ANOVA:F (7,49) = 0.914,p < 0.01]. In addition, the Sirtinol 10 group experienced a more significant increase in NEFL levels than the icariin 30 group. Nevertheless, when icariin 30 and Sirtinol 10 are used together, NEFL levels decrease significantly more than when Sirtinol 10 is used alone (Fig. 4C).

*3.1.6.6. Icariin-mediated neuroprotective potential reduces TDP43 aggregation in experimental ALS rats.* The concentration of TDP 43 in CSF and blood plasma was measured using an ELISA kit. Compared to the control, vehicle, and icariin 30 perse groups, TDP 43 levels increased significantly after long-term MeHg 5 administration. In conclusion, continued administration of icariin 15 and icariin 30 decreased TDP 43 levels in brain homogenate [one-way ANOVA: F (7,49) = 2.183,p < 0.01] and CSF [one-way ANOVA:F (7,49) = 2.280,p < 0.01]. With icariin 30, TDP 43 levels decreased substantially more than with icariin 15. In addition, the Sirtinol 10 group experienced a greater increase in TDP 43 levels than the icariin 30 group. TDP 43 levels decrease substantially more when combined with icariin 30 and Sirtinol 10 than when Sirtinol 10 is used alone (Figures D, E).

*3.1.6.7. Icariin-mediated neuroprotective potential modulates neurotransmitter imbalance in experimental ALS rats.* After completing the study protocol, the concentrations of various neurotransmitters were measured. Compared to the control, vehicle, and icariin 30 perse groups, the acetylcholine levels of MeHg 5- treated rodents were significantly lower. Cortex [one-way ANOVA:F (7,49) = 0.537,p < 0.01], Hippocampus [one-way ANOVA:F (7,49) = 0.997, p < 0.01], and Striatum [one-way ANOVA:F (7,49) = 3.177,p < 0.01] showed increases in acetylcholine following continuous administration of icariin 15 and icariin 30 regularly. The icariin 30 group showed significant restoration of neurotransmitter levels, while the Sirtinol 10 group experienced a greater acetylcholine decrease, with the Icariin 30 + Sirtinol 10 treatment group showing superior results. After completing the study protocol, the concentrations of various neurotransmitters were measured. Dopamine levels in MeHg 5 treated rats were significantly lower than in the control, vehicle, and icariin 30 perse groups. Dopamine levels increased in the cortex [one-way ANOVA:F (7,35) = 1.951,p < 0.01], hippocampus [one-way ANOVA:F (7,49) = 1.584,p < 0.01], and striatum [one-way ANOVA:F (7,35) = 3.003,p < 0.01] after continuous administration of icariin 15 and icariin 30 regularly. The study found that the icariin 30 group significantly restored neurotransmitter levels, while the Sirtinol 10-treated group experienced more dopamine levels, and the Icariin 30 + Sirtinol 10 treatment group showed superior results. The concentrations of several neurotransmitters were tested once the study regimen was completed. Compared to the control, vehicle,

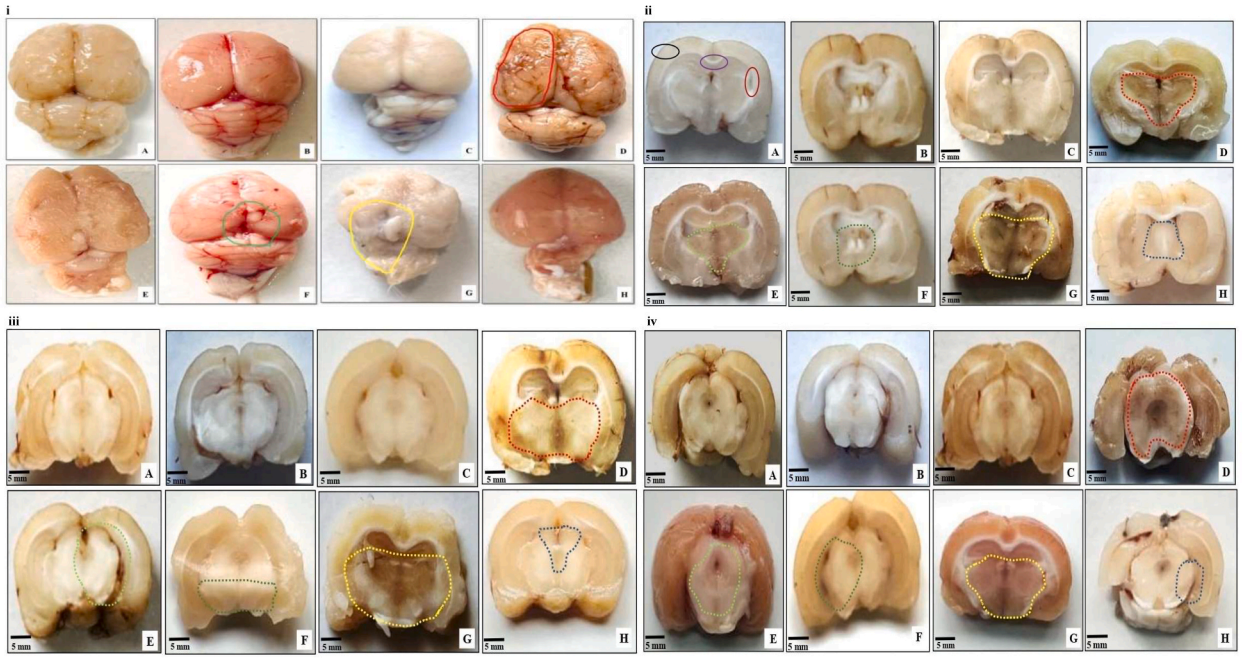


**Fig. 5.** i-iv (A–H): Icariin-mediated neuroprotective potential restore gross pathological alterations, coronal segments, mid-brain segments and cerebellum segments of rat brain, in experimental ALS rats. ***(a)*** *Normal control* ***(b)*** *Vehicle control* ***(c)*** *Icariin 30 perse* ***(d)*** *MeHg 5* ***(e)*** *MeHg 5 + Icariin 15* ***(f)*** *MeHg 5 + Icariin 30* ***(g)*** *MeHg 5 + Sirtinol 10* ***(h)*** *MeHg 5 + Icariin 30 + Sirtinol 10. Note:* ***Red dotted Colour line****: Demyelination in MeHg 5 Group; Green dotted Colour line: Remyelination in Icariin* 30 mg/kg *treated brain;* ***Yellow dotted Colour line****: Sirtinol 10 treated group; The black circle represents Cortex*; *the Purple colour represents Hippocampus*; *the Red colour represents Striatum. [5ii]*. (For interpretation of the references to colour in this figure legend, the reader is referred to the Web version of this article.)

and icariin 30 perse groups, rodents treated with MeHg 5 had significantly lower GABA levels. Cortex [one-way ANOVA:F (7,49) = 0.3613, $p < 0.01$], Hippocampus [one-way ANOVA:F (7,49) = 1.512,$p < 0.01$], and Striatum [one-way ANOVA:F (7,49) = 0.5885,$p < 0.01$] all exhibited increases in GABA following continuous administration of icariin 15 and icariin 30 regularly. The icariin 30 group showed significant restoration of neurotransmitter levels, while the Sirtinol 10 alone-treated group experienced more GABA levels decrease. (Figure F, G, H, I).

*3.1.6.8. Icariin-mediated neuroprotective potential modulates glutamate imbalance in experimental ALS rats.* After the experimental protocol was completed, Glutamate concentrations were measured. Compared to the control, vehicle, and icariin 30 perse groups, rats treated with MeHg 5 had significantly elevated levels of glutamate. Glutamate levels decreased in the cortex [one-way ANOVA:F (7,49) = 1.210,$p < 0.01$], striatum [one-way ANOVA:F (7,49) = 0.290,$p < 0.01$], and hippocampus [one-way ANOVA:F (7,49) = 0.876,$p < 0.01$] after treatment with icariin 15 and icariin 30 continuously. The study found that icariin 30-treated groups significantly increased glutamate levels, while Sirtinol 10 alone resulted in a higher increase (Fig. 4J).

*3.1.6.9. Icariin-mediated neuroprotective potential restores methylmercury levels in experimental ALS rats.* The experiment revealed that the MeHg 5 treatment group had significantly higher MeHg 5 levels than the normal control, vehicle control, and icariin 30 perse groups. Compared to rats exposed to MeHg 5, rats given icariin 15 or icariin 30 orally for an extended period of time had less MeHg 5 in their cerebral tissues [one-way ANOVA:F (7,49) = 0.752,$p < 0.01$]. MeHg 5 levels decreased by a statistically significant margin in the icariin 30-treated group compared to the icariin 15-treated group. The Sirtinol 10-treated group experienced a significant increase in MeHg 5 compared to the icariin 30-treated group. In addition, MeHg 5 levels were substantially lower in the combination treatment group receiving Icariin 30 and Sirtinol 10 compared to the Sirtinol 10 treatment group (Fig. 4K).

*3.1.7. Icariin-mediated neuroprotective potential restores gross pathological alterations in experimental ALS rats*

*3.1.7.1. Icariin-mediated neuroprotective potential restores whole brain of rat brain in experimental ALS rats.* MeHg 5-exposed ALS rats showed brain size fluctuations, decreased weight, and motor neuron damage compared to normal controls. Long-term icariin (15 and

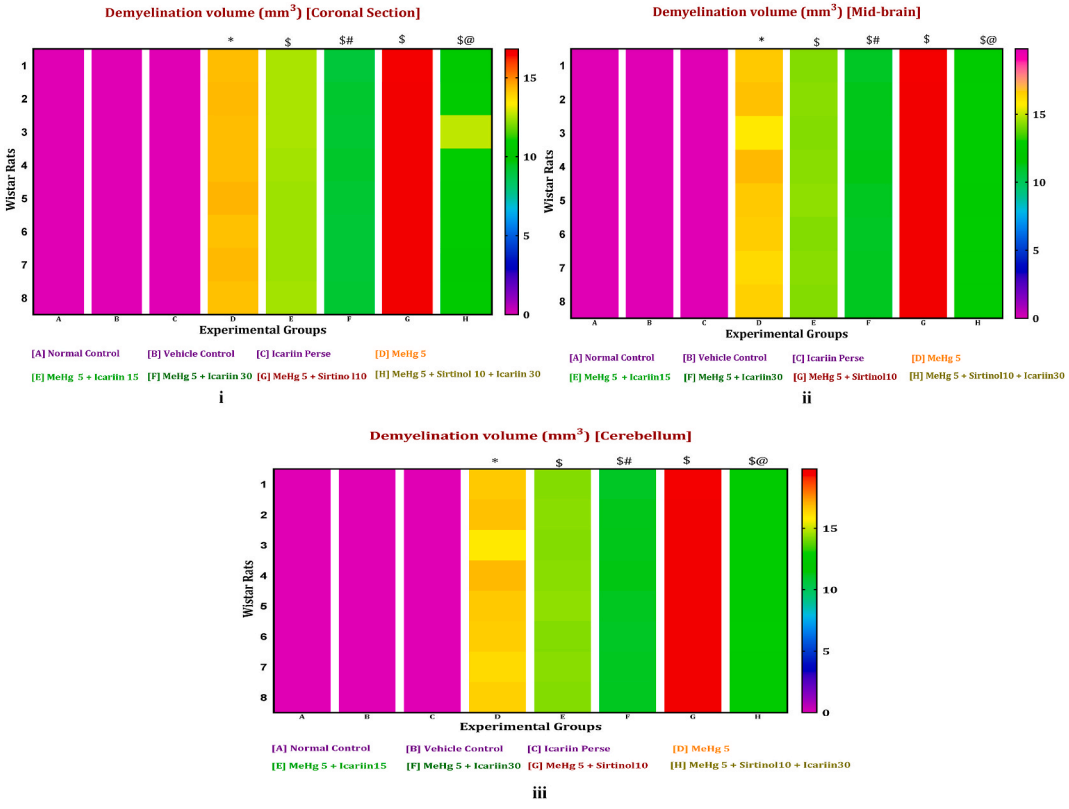


**Fig. 6. (i-iii): Icariin-mediated neuroprotective potential reduces demyelination volume in coronal segments, mid-brain segments and demyelination volume in cerebellum segments of rat brain in experimental ALS rats**. *The statistical data analysis was presented using one-way ANOVA analysis by using Tuckeys test. Values presented as mean ± S. D [n = 8 Wistar rats in each experimental group; $p < 0.01$]. *Versus Normal, Vehicle control and icariin perse control; **$** Versus MeHg 5; **$#** versus icariin 15; and **$@** Versus MeHg 5, Sirtinol 10, icariin 30.* [*6i, 6ii, 6 iii*].

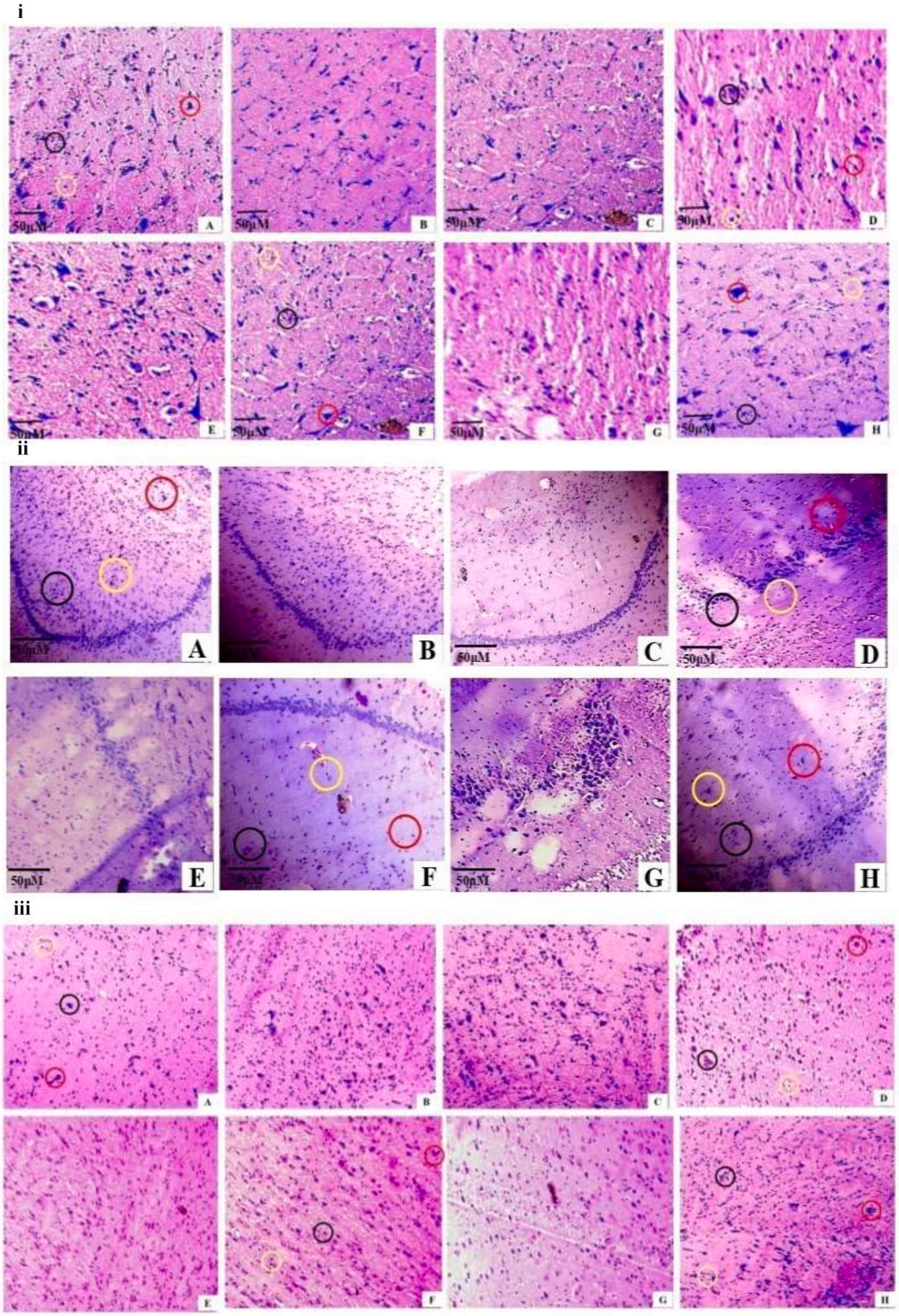


*(caption on next page)*

**Fig. 7. i (A–H): Icariin-mediated neuroprotective potential reduces histopathological changes in experimental ALS rats.** *Under a fluorescence microscope, the chosen panels in the figure depict populations of neurons stained with Hematoxylin and Eosin. During MeHg 5 exposure, icariin, and sirtinol treatment, light microscopy reveals the following morphological modifications in the brain's cortex region: Indicates a cerebral folium with grey matter on the exterior and white matter on the exterior of the interior. Grey matter consists of an outer molecular layer (M), a Purkinje cell layer (P), and an interior granular layer (G). The outermost molecules (M) layer consists of glial cells. In contrast, the middle layer of Grey matter comprises large pyriform Purkinje neuronal cells and Bergmann protoplasmic astrocytes (black circle) (yellow circle). Purkinje cells and Bergmann protoplasmic astrocytes were present, distinct, and long-lasting. Section (b) Vehicle Classifying: The structural layer, the Purkinje section, and the granular section are represented. The integrity of Purkinje cells was not compromised. Like the control group, section (c) of the icariin perse group displays the typical distribution of all layers and neuronal cells. The group treated with methylmercury (d): Visible in the molecular layer (M) are the toxic effects of MeHg 5, as well as areas of degeneration (D) comprised of dispersed and poorly defined oligodendrocyte cells. As indicated by the yellow circle, astrocytes have also lost their structural integrity, joining a significant proportion of oligodendrocytes in leaving behind vacant spaces. (S) and a decrease in nucleus density (Black Circle) are both signs of inflammation. (e) The icariin 15-treated group exhibited a modest restoration of Oligodendrocytes and astrocyte cells, with less clumping (Red circle) (yellow circle) in the inner layer. (f) The icariin 30-treated group demonstrates substantially more reconstruction in the degenerative cortex region, with an increase in vacant desert space (rS), the density of nuclei cells, and clear and sharp protoplasmic astrocytes. Section (g) of the Sirtinol 10-treated group reveals an increase in degeneration in particular regions, with oligodendrocytes and astrocytes becoming entangled or damaged. Section (h) Icariin 30 & Sirtinol 10-treat reveals significantly enhanced overall astrocyte cell strength, significant improvements in oligodendrocytes, and minor nucleus restoration. (Magnification = 40×; Scale = 50 μM).* ***Note:*** *The red circle represents-oligodendrocyte cells; the Yellow circle- Astrocytes; the Black circle- Nucleus density.* ***Fig. 7ii (A-E):*** **Highlights that Icariin can alleviate histopathological changes by minimizing them in the Hippocampus region**. *Neuronal networks are fluorescently stained with Hematoxylin and Eosin in certain figure sections. During MeHg 5 exposure and icariin and sirtinol treatment, light microphotographs revealed the following morphological changes in the hippocampus. The alveus refers to the interior surface of the ventricles of the hippocampus. The alveus, a thin layer of white matter, is formed when the axons of hippocampal pyramidal cells converge. Section (a) Normal control: Indicates the presence of grey matter known as fimbria on the exterior and white matter known as alveus on the interior, both composed of pyramidal hippocampal cells. Oligodendrocytes and astrocytes are depicted as strong and healthy cells. b) Vehicle group: demonstrates that the oligodendrocytes and astrocytes have maintained normal viability. Section (c) icariin perse group: Displays similarities to the control group and the distribution of cells. Section (d) of the MeHg5-treated group reveals a region of degeneration characterized by oligodendrocytes and astrocytes that are unclear, fragmented, and deformed. As the red circle behind the intercellular spaces indicates, all cells have lost their integrity. The MeHg 5 + Icariin 15-treated group exhibits minimal regrowth of oligodendrocytes and a uniform distribution of astrocytes in the region of the hippocampal gyrus (section e). Section (f) MeHg 5 + Icariin 30-treated group: Exhibits a significantly more healing region in the hippocampal pyramidal cells, recovery in the oligodendrocytes and astrocytes cells, and a largely uniform cell arrangement. Comparing the MeHg5-treated group to the MeHg 5 + Sirtinol 10-treated group, the MeHg 5 + Sirtinol 10-treated group was more destructive, with all cells exhibiting abnormal size and morphology. Section (h) of the MeHg 5 + Icariin 30 + Sirtinol 10-treated group demonstrates a partial recovery of the oligodendrocytes and astrocytes that comprise the hippocampus region. (Magnification = 40×; Scale = 50 μM).* ***Note:*** *The red circle represents-oligodendrocyte cells; the Yellow circle represents astrocytes; the Black circle represents nucleus density.* ***Fig. 7iii (A-E): Highlights that Icariin can alleviate histopathological changes by minimizing them in the Striatum region***. Under a fluorescence microscope, the chosen panels in the figure depict populations of neurons stained with Hematoxylin and Eosin. During MeHg 5 exposure and icariin and sirtinol treatment, light micrographs showed the following morphological changes in the midbrain. The caudate nucleus and putamen comprise the dorsal striatum. This section (a) represents a normal brain with grey matter on the exterior and white matter on the interior. The outer molecular layer (M) contains the nucleus (Black circle), while the intermediate oligodendrocytes cell layer contains large pyriform neuronal cells and extracellular matrix astrocytes (Yellow and red circles, respectively). Both oligodendrocytes and astrocytes were considered whole, differentiated, and well-organized. Section b, Group of Vehicles, depicts a typical molecular, Purkinje, and granular layer structure. There was no change in the structural integrity of oligodendrocytes. The icariin perse group exhibits the same uniform arrangement of neuronal cells and cellular layers as the control group. MeHg 5 group: section (d) in the molecular layer (M), the toxic effects of MeHg 5 are visible as areas of degeneration (d) composed of dispersed and poorly defined oligodendrocytes. The red circle represents a damaged astrocyte that, like most oligodendrocytes, has left behind vacant spaces and decreased nucleus density (black circle), indicating inflammation. Section (e): The MeHg 5+ Icariin 15 treated group displays a slight restoration of oligodendrocytes and astrocytes and a reduction in internal layer clustering. Section (f) MeHg 5+ Icariin 30-treated group: Significantly more reconstruction in the degenerative area of the mid-brain region, with an increase in vacant desert space (rS), the density of nuclei cells, and the number of pointed and evident protoplasmic astrocytes. Section (g) of the MeHg 5+ Sirtinol 10-treated group reveals oligodendrocyte degeneration in specific locations. Astrocyte cells are dispersing or being destroyed. Section (h) of the MeHg 5+ Icariin 30 and Sirtinol 10 treated group demonstrates the minimal restoration and regeneration of oligodendrocytes. (Magnification = 40×; Scale = 50 μM). **Note:** The red circle represents-oligodendrocyte cells; the Yellow circle represents astrocytes; the Black circle represents nucleus density. (For interpretation of the references to colour in this figure legend, the reader is referred to the Web version of this article.)

30) treatment increased brain mass and reduced pathology, with icariin 30 being more effective than icariin 15. Sirtinol 10 treatment also decreased pathology, and the combination of icariin 30 and Sirtinol 10 further improved brain morphology, indicating icariin 30's superior effectiveness. Fig. 5i (A-H).

*3.1.7.2. Icariin-mediated neuroprotective potential restores coronal segments of rat brain in experimental ALS rats.* Normal, vehicle control and icariin 30 perse-treated rats showed acceptable cortex, hippocampus, and striatum tissue quality in brain sections. MeHg 5-treated rats had significantly less tissue in these areas. Icariin treatment (15 and 30) significantly improved demyelination and pathological changes in coronal sections. Sirtinol 10 alone reduced brain size and morphology, but combining it with icariin 30 significantly lessened degenerative changes compared to Sirtinol 10 alone. Fig. 5ii (A-H).

*3.1.7.3. Icariin-mediated neuroprotective potential restores mid-brain segments of rat brain in experimental ALS rats.* In our study, the midbrain tissue of rats treated with icariin 30 showed transparency and high quality. Rats exposed to MeHg+ exhibited significant midbrain tissue reduction, while icariin treatment (15 and 30) reduced demyelination and pathological changes. Treatment with

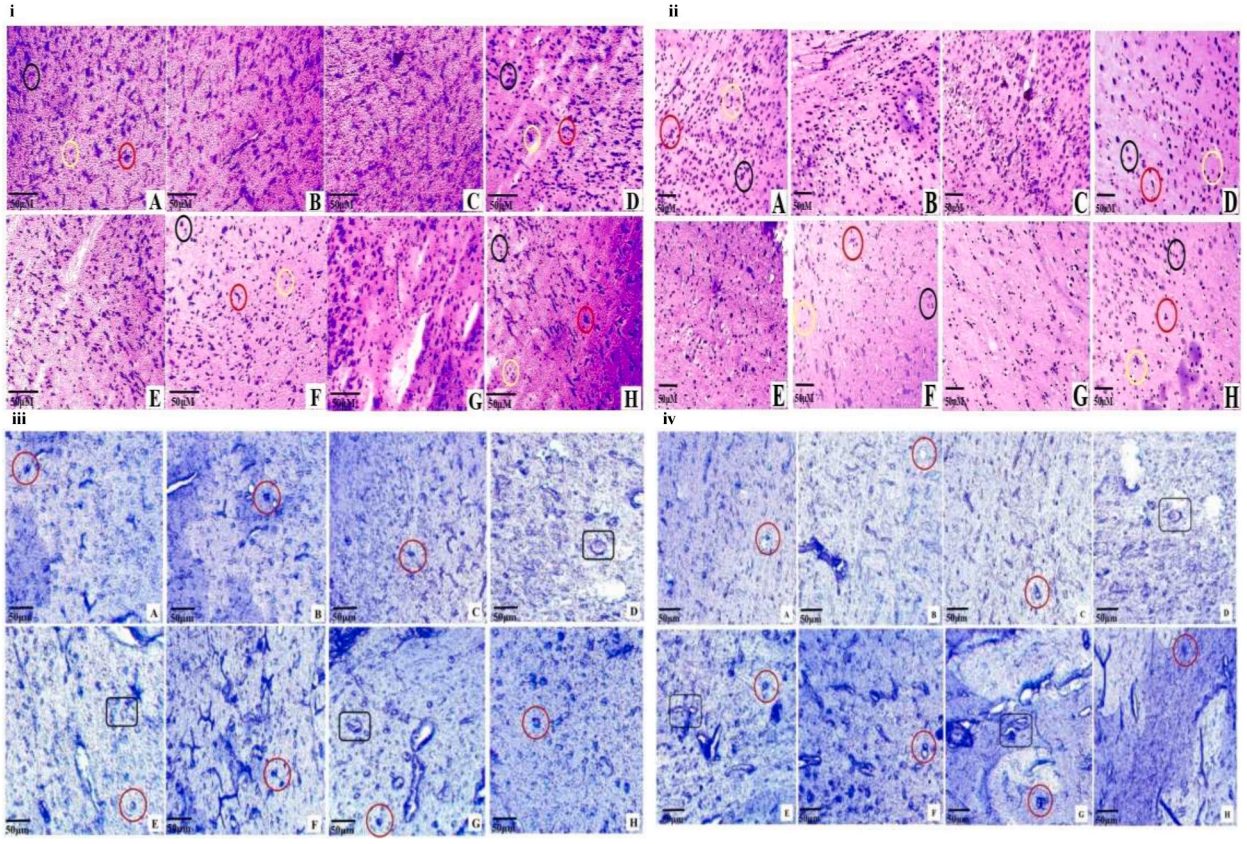


*(caption on next page)*

**Fig. 8.** i (A–H): Highlights that Icariin can alleviate histopathological changes by minimizing them in the midbrain region. The chosen panels show populations of neurons dyed with Hematoxylin and Eosin using a fluorescent microscope. During MeHg 5 exposure and icariin, sirtinol treatment, light micrographs revealed the subsequent morphological changes in the midbrain: The brain's periaqueductal grey (PAG) region is essential for the processing of pain signals, autonomic regulation, and the behavioral manifestation of fear and anxiety. This section (a) represents a normal brain with grey matter on the exterior and white matter on the interior. The outer molecular layer (M) contains the nucleus (Black circle), while the intermediate oligodendrocytes cell layer contains large pyriform neuronal cells and extracellular matrix astrocytes (Yellow and red circles, respectively). Both oligodendrocytes and astrocytes were considered whole, differentiated, and well-organized. Section b, Group of Vehicles, depicts a typical molecular, Purkinje, and granular layer structure. There was no change in the structural integrity of oligodendrocytes. The icariin perse group exhibits the same uniform arrangement of neuronal cells and cellular layers as the control group. MeHg 5 group: section (d) In the molecular layer (M), the toxic effects of MeHg 5 are visible as areas of degeneration (d) composed of dispersed and poorly defined oligodendrocytes. The red circle represents a damaged astrocyte, which, along with most oligodendrocytes, has left behind voids, and a decrease in nucleus density (Black circle) are two indicators of inflammation. Section (e): The MeHg 5+ Icariin 15-treated group displays a slight restoration of oligodendrocytes and astrocytes and a reduction in internal layer clustering. Section (f) MeHg 5+ Icariin 30-treated group: Significantly more reconstruction in the degenerative area of the mid-brain region, with an increase in vacant desert space (rS), the density of nuclei cells, and the number of pointed and clear protoplasmic astrocytes. Section (g) of the MeHg 5+ Sirtinol 10-treated group reveals oligodendrocyte degeneration in specific locations. Astrocyte cells are dispersing or being destroyed. Section (h) of the MeHg 5+ Icariin 30 and Sirtinol 10 treated group demonstrates the minimal restoration and regeneration of oligodendrocytes. (Magnification = 40×; Scale = 50 μM). **Note:** Red circle represent-oligodendrocyte cells; Yellow circle- Astrocytes; Black circle- Nucleus density. ***Fig. 8ii (A-H): Highlights that Icariin can alleviate histopathological changes by minimizing them in the cerebellum region****. Under a fluorescence microscope, the panel in the figure was chosen to illustrate a neuronal population stained with Hematoxylin and Eosin. Fluorescence micrographs revealed the following changes in the cerebellum following exposure to MeHg 5, icariin, and sirtinol: Group (a): Represent a cerebellum with the grey matter on the exterior and white matter on the interior. The grey matter comprises three distinct layers: The outermost layer of molecules (M) and the interior layer of granules (G). The outer molecular layer (M) contains the nucleus (Black circle), while the intermediate oligodendrocytes cell layer contains large pyriform neuronal cells and extracellular matrix astrocytes (Yellow and red circles, respectively). Oligodendrocytes and astrocytes were found to be wholly distinct and well-organized. Section b, Group of Vehicles, depicts a typical molecular, Purkinje, and granular layer structure. Oligodendrocytes maintain the integrity of their structures. Section (C) icariin perse group: Displays a typical arrangement of all layers and neuronal cells, similar to the control group. Section (d) of the MeHg 5- treated group demonstrates the toxic effect of MeHg 5 in the molecular layer (M) with areas of degeneration (D) characterized by oligodendrocyte cells that have lost their integrity, leaving empty spaces (S) with a decrease in nucleus density (Black circle) that was distributed, indicating inflammation, and astrocytes that have lost their integrity, as shown by the Red circle. The (e) section of the icariin 15-treated group displays a modest recovery of oligodendrocytes. Section (f) of the icariin 30-treated group displays significantly more reconstruction of oligodendrocytes and astrocyte cells, with clumping being reduced (Yellow circle) in the inner layer and restoration in the degenerative areas, as well as an increase in empty spaces (rS) and density of nuclei cells, as well as a rise in clear and sharp protoplasmic astrocytes. Compared to the MeHg 5 treated group, oligodendrocytes and astrocytes in section (g) of the MeHg 5 + Sirtinol 10-treated group exhibit more significant degeneration. Section (h) of the MeHg 5 + Icariin 30 + Sirtinol 10- treated group reveals a modest recovery of nuclei and astrocytes. (Magnification = 40×; Scale = 50 μM). **Fig. 8iii (A-H): Icariin-mediated neuroprotective potential improves LFB- Stained demyelinated midbrain part in experimental ALS rats****. Myelin stained with LFB dye appears blue in representative fluorescent micrographs. LFB staining, used to examine degeneration in the Midbrain area using a microscope, was chosen as the technique for staining. Section (a) usually represents functioning myelinated neurons; (b) represents the Vehicle group; and (c) represents the icariin 30 perse group. Toxic consequences of MeHg 5 are seen in section (d) for the MeHg 5-treated group, where the black box represents an increasing region of demyelination. Myelin sheath degradation products are consumed by macrophages, a hallmark of neuroinflammation (red circle). (e) MeHg 5 + Icariin 15: The group partially restored Demyelination and engulfment of macrophages. Group (f) MeHg 5 + icariin 30 shows reduced demyelination and fewer macrophages, indicating more clear and undamaged nerve cells. In group (g) MeHg 5 + Sirtinol 10, demyelination was repaired, and fewer macrophages were present in the part examined. Eventually, the treatment of MeHg 5 for 21 days leads to a decline in neuroinflammation, as evidenced by the more precise and well-structured presence of myelinated nerve cells in the MeHg 5 + icariin 30 + Sirtinol 10 group {see section (h)}, with an area more of remyelination than demyelination (as shown by the black box) and fewer macrophages. **Fig. 8iv (A-H): Icariin-mediated neuroprotective potential improves LFB- Stained demyelinated Cerebellum brain part in experimental ALS rats****. Blue fluorescence is observed in fluorescent micrographs of myelin stained with LFB dye. The LFB staining method was used since it is commonly used to examine degeneration in the cerebellum region under a microscope. Part (a) depicts myelinated neurons that are operating normally, Part (b) depicts the vehicle group, and Part (c) depicts the icariin 30 perse group. In section (d), where the black box depicts an expanding demyelinated region, the toxic effects of MeHg 5 are seen in the MeHg 5-treated group. A characteristic of neuroinflammation is the consumption of byproducts of myelin sheath breakdown by macrophages (red circle). Demyelination and macrophage engulfment were partially recovered in group (e) MeHg 5 + icariin 15. Reduced demyelination and fewer macrophages in group (f) MeHg 5 + Icariin 30 indicate more intact and clean nerve cells. Demyelination was restored, and macrophage numbers were reduced in group (g) MeHg 5 + sirtinol 10. After 21 days of MeHg 5 + treatment, neuroinflammation decreases, as seen by a greater proportion of remyelination over demyelination (as depicted by the black box) and a general decrease in the number of myelinated nerve cells (see Section (h))*. (For interpretation of the references to colour in this figure legend, the reader is referred to the Web version of this article.)

sirtinol alone reduced brain size and morphology, but combining icariin 30 and sirtinol 10 significantly improved the midbrain's appearance compared to sirtinol treatment alone. Fig. 5iii (A-H).

*3.1.7.4. Icariin-mediated neuroprotective potential restores cerebellum segments of rat brain in experimental ALS rats.* Normal, vehicle control and icariin 30 perse-treated rat brain sections showed satisfactory cerebellum tissue quality. MeHg 5-treated rats had a notably smaller cerebellum. Treatment with icariin 15 and 30 significantly improved demyelination and pathology in the cerebellum. Sirtinol 10 alone reduced brain size and shape, but combining it with icariin 30 notably lessened cerebellar degeneration compared to Sirtinol 10 alone. Fig. 5iv (A-H).

*3.1.7.5. Icariin-mediated neuroprotective potential reduces demyelination volume in coronal segments of rat brain in experimental ALS rats.* The extent of degeneration in coronal segments did not differ significantly between the normal control, vehicle control, and icariin 30 perse groups. In both coronal sections, the demyelination area was substantially larger in the MeHg 5 administration for 21 days group compared to the control, vehicle, and icariin 30 perse treatment groups. In addition, prolonged treatment with icariin 15 and icariin 30 significantly reduced demyelination compared to groups that only received MeHg 5 in the coronal section [one-way ANOVA: $F(7,35) = 1.262, p < 0.01$]. In contrast to the icariin 30-treated group, the Sirtinol 10-treated group exhibited a significant increase in demyelination volume. Comparatively to the Sirtinol 10 group, combining icariin 30 and Sirtinol 10 significantly reduced demyelination in both coronal regions (Fig. 6i).

*3.1.7.6. Icariin-mediated neuroprotective potential reduces demyelination volume in mid-brain segments of rat brain in experimental ALS rats.* There was no significant difference in the magnitude of degeneration regions in midbrain sections between the normal control, vehicle control, and icariin 30 perse groups. MeHg 5 administration for 21 days resulted in substantially more demyelination in both midbrain sections compared to the control, vehicle, and icariin 30 per se groups. In addition, when compared to groups that only received MeHg 5 in the midbrain region, icariin 15 and icariin 30 treatment for longer durations significantly decreased the demyelination area [one-way ANOVA:$F(7,35) = 1.623, p < 0.01$]. In contrast, the midbrain sections of the Sirtinol 10-treated group exhibited a striking increase in demyelination volume. In contrast to the Sirtinol 10 group, the volume of demyelination in midbrain sections was substantially reduced in the icariin 30 and Sirtinol 10 combination groups (Fig. 6ii).

*3.1.7.7. Icariin-mediated neuroprotective potential reduces demyelination volume in cerebellum segments of rat brain in experimental ALS rats.* There was no significant difference in the size of degeneration regions on cerebellum sections between the normal control, vehicle control, and icariin 30 perse groups. The demyelination in both cerebellar portions was significantly greater when MeHg 5 was administered for 21 days versus the normal, vehicle, and icariin 30 perse treatment groups. Moreover, compared to groups that only received MeHg 5 in the cerebellar region, longer periods of icariin 15 and icariin 30 therapy reduced the demyelination area significantly [one-way ANOVA:$F(7,35) = 1.623, p < 0.01$]. The Sirtinol 10 alone treated group demonstrated a significant increase in demyelination volume in cerebellar sections. The volume of demyelination in cerebellum sections was drastically reduced in the icariin 30 and Sirtinol 10 combination group compared to the Sirtinol 10 group (Fig. 6iii).

*3.1.8. Icariin-mediated neuroprotective potential reduces histopathological changes in experimental ALS rats*

*3.1.8.1. In cortex region.* Treatment groups showed varying effects on the Purkinje cell layer in the rat cortex. The MeHg 5 group exhibited fewer, less distinct Purkinje cells and increased neuroinflammation with higher microglia density. Icariin treatment enhanced Purkinje cells, reduced microglial density, and improved Bergmann protoplasmic astrocytes in a dose-dependent manner. Sirtinol 10 administration led to more degraded Purkinje cells, fewer Bergmann astrocytes, and increased neuroinflammation. However, combining icariin with Sirtinol 10 reversed MeHg 5-induced neurotoxicity by improving cell visibility and reducing degeneration. Fig. 7i (A-H).

*3.1.8.2. In hippocampus region.* Treatment groups impacted the Purkinje cell layer differently. The MeHg 5 group had fewer, less distinct Purkinje cells with increased neuroinflammation and abnormal microglia and astrocyte densities. Icariin improved Purkinje cell clarity and reduced microglial density, while sirtinol 10 led to more damaged Purkinje cells and increased microglial density. However, combining icariin with Sirtinol 10 reversed these effects, preventing cell death and improving cell visibility in the rat hippocampus. Fig. 7ii (A-H).

*3.1.8.3. In striatum region.* Treatment groups variably affected the Purkinje cell layer. In the MeHg 5 group, Purkinje cells were fewer and less distinct, with increased microglia density due to CNS inflammation. Icariin improved Purkinje cell sharpness and astrocyte health, while sirtinol 10 increased microglial density and Purkinje cell damage. However, combining icariin with sirtinol 10 effectively reversed MeHg 5-induced neurotoxicity in the rat striatum. Fig. 7iii (A-H).

*3.1.8.4. Icariin-mediated neuroprotective potential reduces histopathological changes in the mid-brain region of experimental ALS rats.* The MeHg 5 group showed a significant reduction in Purkinje cells and increased microglia density due to CNS inflammation, with notable structural abnormalities. Icariin improved Purkinje cell clarity, microglial density, and astrocyte health, whereas sirtinol 10 led to more Purkinje cell damage and increased microglia. However, combining icariin with sirtinol 10 reversed MeHg 5-induced neurotoxicity in the rat midbrain. Fig. 8i (A-E).

*3.1.8.5. Icariin-mediated neuroprotective potential reduces histopathological changes in the cerebellum region of experimental ALS rats.* All treatment groups altered the oligodendrocyte layer. The MeHg 5 group showed significantly fewer and less differentiated oligodendrocytes, with increased microglia density due to CNS inflammation. Icariin improved oligodendrocyte clarity and astrocyte function, whereas sirtinol 10 led to more damage and increased microglia. Combining icariin and sirtinol 10 effectively reversed MeHg 5-induced neurotoxicity in the rat cerebellum, enhancing cell survival and visibility. Fig. 8ii (A-E).

*3.1.8.6. Icariin-mediated neuroprotective potential improves LFB-Stained demyelinated midbrain part in experimental ALS rats.* LFB staining showed a normal nerve cell distribution in the control, vehicle, and icariin perse groups. However, MeHg5 exposure significantly altered this pattern, leading to myelin sheath degradation and widespread demyelination. Icariin 15 and 30 treatments reduced macrophages and demyelination, while Sirtinol 10 alone showed typical degeneration. The combination of icariin 30 and Sirtinol 10 was more effective in reversing MeHg 5 toxicity in rat brains. Fig. 8iii (A-H).

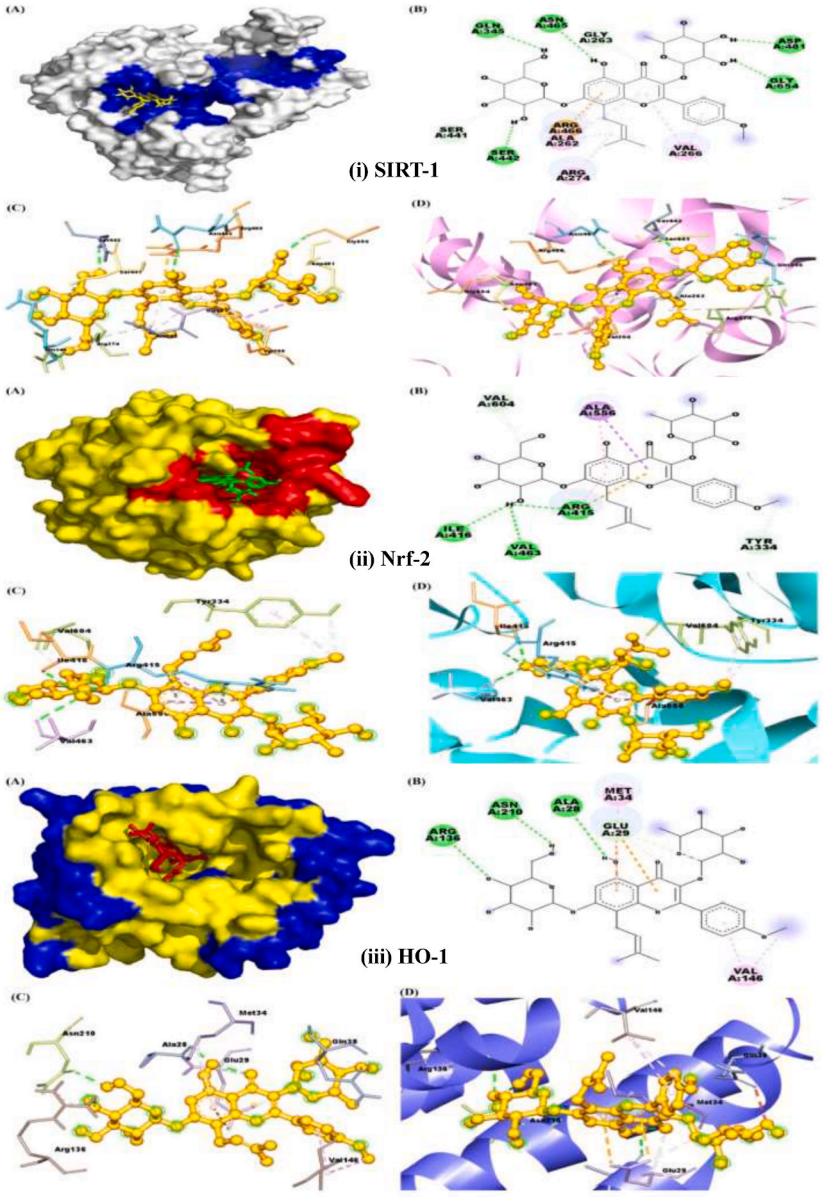


**Fig. 9. (i) SIRT-1** *(A) Surface mapping of protocol drug icariin yellow colour in the cavity of SIRT-1 receptor (PDB ID: 5BTR) (B) Showing 2D interactions view of icariin with the SIRT-1 receptor (PDB ID: 5BTR). (C) 3D view of icariin in golden colour participating in the interactions with the residues of SIRT-1 receptor (PDB ID: 5BTR) (D) icariin golden colour showing stable ligand interactions with the active sites of the SIRT-1 receptor (PDB ID: 5BTR).* **Fig. 9(ii) Nrf-2** *(A) Surface mapping of protocol drug icariin green color in the cavity of Nrf-2 receptor (PDB ID:5CGJ) (B) Showing 2D interactions view of icariin with the Nrf-2 receptor (PDB ID:5CGJ). (C) 3D view of icariin in golden colour participating in the interactions with the residues of NRF-2 receptor (PDB ID:5CGJ) (D) icariin golden colour showing stable ligand interactions with the active sites of the NRF-2 receptor (PDB ID:*5CGJ). **Fig. 9(iii)OH-1** *(A) Surface mapping of protocol drug icariin red colour in the cavity of HO-1 receptor (PDB ID: 3HOK) (B) Showing 2D interactions view of icariin with the HO-1 receptor (PDB ID: 3HOK). (C) 3D view of icariin in golden colour participating in the interactions with the residues of HO-1 receptor (PDB ID: 3HOK) (D) icariin golden colour showing stable ligand interactions with the active sites of the HO-1 receptor (PDB ID*: 3HOK). (Fig. 9A–D). (For interpretation of the references to colour in this figure legend, the reader is referred to the Web version of this article.)

*3.1.8.7. Icariin-mediated neuroprotective potential improves LFB-stained demyelinated cerebellum brain part in experimental ALS rats.* In fluorescent micrographs, myelin stained with LFB dye appears blue, indicating demyelination in the cerebellum. Sections show various treatments: (a) normal myelinated neurons; (b) Vehicle group; (c) Icariin 30 perse; and (d) MeHg 5 with increased demyelination (black box) and neuroinflammation (red circle). Group (e) MeHg 5 + icariin 15 and (f) MeHg 5 + icariin 30 exhibit reduced demyelination and macrophages, while group (g) MeHg 5 + sirtinol 10 shows repaired demyelination. The combination in group (h) MeHg 5 + icariin 30 + sirtinol 10 significantly lessens neuroinflammation and enhances remyelination. Fig. 8iv (A-H).

*3.1.8.8. In sillico validation studies: icariin-mediated target interaction.* The affinity scores of the protocol drug icariin for (PDB ID: 3HOK), (PDB ID: 5CGJ), and (PDB ID: 5BTR) were observed as −7.7, −8.7, and −8.7 kcal/mol respectively. The ligand efficiency (LE) of icariin for the selected targets was found to be 0.219, 0.248, and 0.248 respectively. Icariin demonstrated the lowest binding affinity for (PDB ID: 5CGJ), and (PDB ID: 5BTR) as compared to (PDB ID: 3HOK). In the protein structure with (PDB ID: 3HOK), the residues Arg136, Asn210, and Ala28 were observed to form hydrogen bonds with icariin. Moving on to the protein structure with (PDB ID: 5CGJ), the residues Ile416, Val463, Arg415, Val604, and Tyr334 were found to exhibit hydrogen bonds with icariin. Similarly, in the protein structure with (PDB ID: 5BTR), the residues Gln345, Asn465, Ser442, Gly654, and Asp481 were identified as participating in hydrogen bonding interactions with icariin. These observations highlight the specific molecular interactions between icariin and these residues within each respective protein structure, providing valuable insights into the binding mechanism and potential biological implications of icariin. The docking poses of the icariin with the selected target (PDB ID: 3HOK), (PDB ID: 5CGJ), and (PDB ID: 5BTR) analyzed with 2D interactions as shown in (Fig. 1), (Fig. 2) and (Fig. 3). The docking results demonstrated that icariin forms stable interactions and favourable binding energies with the active sites of these receptors, and a detailed analysis of the binding sites of SIRT-1, Nrf-2, and HO-1 receptors reveals crucial interactions with icariin. These interactions suggest a potential activation mechanism for these receptors. In-silico studies demonstrated the conformational changes induced by icariin binding to the SIRT-1, Nrf-2, and HO-1 receptors. These conformational alterations may play a role in the activation of these receptors in the signaling pathways (Fig. 9A–D).

## 4. Discussion

ALS, an incurable disease, leads to paralysis and respiratory failure from motor function deterioration. Urgent development of treatments to slow progression and improve life quality is needed. Dysfunctional astrocytes and oligodendrocytes in ALS secrete harmful substances, exacerbating motor neuron loss and myelin damage [64,65]. Demyelination in ALS reduces neuronal connectivity, worsening the disease [66]. Understanding ALS's mechanisms, including motor neuron degeneration and genetic factors, is crucial. Exploring nutraceuticals and plant-based drugs, like icariin, is promising for treating the complexity of ALS [1,4,5]. The role of cellular markers like SIRT-1, Nrf-2, and HO-1 in ALS progression remains underexplored. Our research also seeks to establish whether SIRT-1, Nrf-2/HO-1, and MBP levels can be diagnostic markers for ALS. Through our research, we examined the phytoconstituent icariin, which has been utilized in the treatment of various neurodegenerative and neuropsychiatric disorders, including AD [67–71], Bipolar disorders [72], Ischemic Stroke [73], PD [14], and Schizophrenia [36].

Icariin, from the Epimedium plant, shows promise in neurodegenerative disorder research due to its neuroprotective properties [70,74]. It can shield neurons from damage and death and has been shown to reduce oxidative stress, inflammation, and apoptosis in the brain, factors crucial in neurodegenerative disease progression [75,76]. There are few investigations on the therapeutic efficacy of icariin in mediating SIRT-1, Nrf-2, and HO-1 in ALS [77,78]. In the present investigation, we aimed to determine how icariin 's modification of these signaling pathways may impact the treatment of behavioral and neurochemical abnormalities in a Wistar rat model of ALS induced by MeHg+. Reducing the protein levels of SIRT-1, Nrf-2, and HO-1 in ALS rats by administering MeHg+ for 21 days resulted in multiple neurodegenerative complications [11,19,39]. Animal and cell studies show that MeHg+ administration accelerates ALS progression. Similar to human exposure, MeHg+ accumulates in rat brains, particularly in the midbrain and cerebellum, damaging oligodendrocytes and affecting myelin integrity [9]. Demyelination in ALS leads to reduced neuronal connectivity [1]. We measured various markers, cytokines, and neurotransmitters in rat brain, blood plasma, and CSF, and conducted histological exams of the brain, including coronal and midbrain sections, using LFB staining to identify demyelination [79,80]. The basal ganglia, crucial for motor control, cognition, and emotion, have direct and indirect neural pathways key to movement control, linked to disorders like ALS [81,82]. These pathways are necessary for regulating motor output, start and stop movements. Imbalances in these circuits, especially in ALS patients exposed to heavy metals like MeHg+, can lead to motor issues and are associated with glutamate dysregulation, motor neuron degeneration, and excitotoxicity [83–85].

In ALS, excess glutamate leads to motor neuron damage, inflammation, and oxidative stress, contributing to neurodegeneration. Increased glutamate release and impaired reuptake in ALS cause accumulation, resulting in excitotoxicity and neuronal injury by overstimulating motor neurons [86,87]. In ALS patients, glutamate levels are higher in areas like the motor cortex and hippocampus [88]. Our research shows that icariin reduces glutamate levels while sirtinol increases them. ALS may also impact other cells and systems, like dopaminergic neurons in the nigrostriatal pathway, due to dysfunctional astrocytes and microglia causing inflammation and releasing toxic substances [46]. Neurotransmitters like acetylcholine, dopamine, and serotonin are implicated in ALS, potentially influencing symptoms like muscle paralysis and cognitive changes [89,90]. Fluctuating serotonin levels in ALS patients affect mood, appetite, sleep, and motor control. GABA, the brain's primary inhibitory neurotransmitter, regulates the balance between excitation and inhibition in neuronal circuits [91,92]. GABA-emitting interneurons are linked to ALS, regulating motor neuron activity [1,4]. MeHg+ exposure causes neurotransmitter decline, but treatment with icariin corrects concentrations, increasing neurotransmitter levels. SIRT-1 expression and activity in ALS-affected tissues may be altered, leading to increased neuronal susceptibility to stress and oxidative damage. Impaired

Nrf-2 signaling in ALS may increase inflammation and neurodegeneration. HO-1, a crucial enzyme in cellular defense against oxidative stress and inflammation, is particularly relevant in ALS [93]. The SIRT-1, Nrf-2, and HO-1 pathway is involved in oligodendrogenesis, inflammatory neurological disorders, and neural activity. Disrupting this pathway could shorten neurocomplications associated with ALS. Rats treated with MeHg+ showed decreased levels of these markers. Oral administration of icariin increased SIRT-1, Nrf-2, and HO-1 levels, suggesting icariin may modulate dysregulation in diseased neural cell types. TDP-43, or TAR DNA-binding protein 43, is a crucial protein in ALS that regulates gene expression and RNA splicing [94,95]. It accumulates in neurons' cytoplasm, producing inclusion bodies, which disrupt cellular processes and potentially cause neuron death [96,97]. The study found that TDP-43 levels were higher after MeHg+ administration and lower after icariin 30 treatment than icariin 15. The reduction was more pronounced in the Sirtinol10-alone treatment group. However, when icariin 30 and Sirtinol 10 were combined, TDP 43 levels decreased, suggesting icariin can be used as a neuroprotective substance. Post-mortem examination of ALS patients' spinal cords showed decreased MBP levels. Long-term MeHg+ treatment significantly decreased MBP levels, while Icariin 15 and icariin 30 led to significant recovery. Sirtinol 10 decreased MBP levels more, while Icariin 30 increased them. Studies show ALS patients have less white matter volume compared to healthy controls. Icariin treatment reverses brain morphological defects and reduces pathology in areas like the cerebral cortex [98]. Our research found that combining icariin with Sirtinol results in dose-dependent myelin regeneration and reduced demyelination compared to Sirtinol alone. Neuronal inflammation is a key factor in ALS pathogenesis, with cytokine-induced inflammation playing a role [99,100]. MeHg+ administration increases pro-inflammatory cytokines like TNF-alpha and IL-1 beta in rats. However, icariin treatment reduces these elevated cytokine levels, particularly when icariin and sirtinol are combined. As scaffolding molecules in the axonal cytoskeleton, neurofilaments serve as neuronal filaments. As a result of axonal degeneration, NEFL is readily released into body fluids [101–103]. In ALS, NEFL plays a crucial role in the pathogenic processes that lead to neuronal inclusion bodies, axonal mutagenesis, and neuronal mortality [5]. Compared to controls, CSF and brain homogenate samples from ALS patients contained more significant quantities of NEFL [104]. Researchers found evidence that NEFL contributed to the development of ALS using a rodent model. The study found that MeHg+ increased NEFL levels in various brain regions, but icariin, an oral drug, reduced them. Sirtinol 10, an antagonist, increased NEFL levels. Combining icariin 30 and Sirtinol 10 significantly restored levels. ALS significantly affects the cerebellum and Midbrain, leading to unbalanced sensory integration and motor coordination [105,106]. MeHg+ disrupts neuronal densities and shrinks Purkinje cells, affecting impulse distribution and synaptic cell coordination. MeHg+ stimulates astrocyte, purkinje, and microglial cell proliferation, affecting the density of intact purkinje cells and neuronal cell integrity. Icariin and Siritnol 10 enhance Purkinje neuronal integrity, while icariin 30 and Siritnol 10 decrease these cells. OPCs usually proliferate and remyelinate neurons after injury, but chronic exposure to neurotoxins like MeHg hampers this process, leading to expanded demyelination and myelin sheath destruction. Studies indicate significant demyelination in rodent ALS models, especially in the corpus callosum, following MeHg+ exposure [1,4,46]. Our research, using fosmid and LFB staining, shows increased myelin repair in icariin-treated rodents, suggesting that icariin may reduce demyelination or enhance myelin repair, especially when combined with Sirtinol. In ALS animal models, weight loss is common due to muscle paralysis and atrophy from motor neuron degeneration [42]. In our study, icariin administration at doses of 15 and 30 showed neuroprotective effects against motor disorders in MeHg+-induced rats, leading to gradual weight restoration and increased body weight, especially when icariin and Sirtinol were used together. The study found that sustained icariin 30 significantly improved grip strength in rats with ALS, a neurodegenerative condition characterized by muscle paralysis and loss of grip strength. However, when Sirtinol 10 was administered alone, the brain-to-body ratio decreased, while when combined with Icariin 30, grip strength increased significantly. The study found that icariin 15 and 30 reduced immobility time in rats, while Sirtinol 10, an antagonist against SIRT-1, Nrf-2, and HO-1, increased immobility time. The open field test and sustained icariin showed significant improvements from day 28 to day 42, indicating a neuroprotective effect on cognitive function recovery [107,108]. The Morris water maze test, which evaluates spatial learning and memory, showed that icariin decreased escape latency by implementing a spatial navigation challenge. Combining icariin 30 and Sirtinol 10 was more effective than either compound alone. The results of the study showed the affinity scores and LE of icariin for three different target proteins, namely SIRT-1 (PDB ID: 5BTR), Nrf-2(PDB ID: 5CGJ), and HO-1(PDB ID: 3HOK). The affinity scores were observed as −7.7, −8.7, and −8.7 kcal/mol, while the LE values of icariin for the selected targets were determined to be 0.219, 0.248, and 0.248, respectively. These LE values provide insights into the effectiveness of icariin as a ligand for the specific targets under investigation. LE is a metric used to assess the binding efficiency of a compound to its target, taking into account both the potency and size of the molecule. Higher LE values indicate a more efficient use of molecular size to achieve binding affinity, suggesting that icariin demonstrates favourable binding characteristics for the three selected targets.

Comparing the binding affinity of icariin across the three protein structures, it can be seen that icariin exhibited the lowest affinity for (PDB ID: 5CGJ) and (PDB ID: 5BTR), as compared to (PDB ID: 3HOK). This suggests that icariin may have a stronger binding interaction with the protein structure represented by (PDB ID: 3HOK).

Further analysis revealed the specific molecular interactions between icariin and the residues within each protein structure. In (PDB ID: 3HOK), icariin formed hydrogen bonds with Arg136, Asn210, and Ala28. In (PDB ID: 5CGJ), icariin exhibited hydrogen bonds with Ile416, Val463, Arg415, Val604, and Tyr334. Similarly, in (PDB ID: 5BTR), icariin formed hydrogen bonds with Gln345, Asn465, Ser442, Gly654, and Asp481. These hydrogen bonding interactions provide valuable insights into the binding mechanism of icariin with each respective protein structure.

The study found stable interactions and favourable binding energies between icariin and SIRT-1, Nrf-2, and HO-1 receptors, suggesting a potential activation mechanism for these receptors. The study highlights the potential of icariin as a drug candidate targeting SIRT-1, Nrf-2, and HO-1 receptors. It suggests that icariin's binding to these receptors induces conformational changes, potentially modulating their activity in signaling pathways. This underscores the need for further research to explore its therapeutic benefits in ALS treatment. Icariin's effects on SIRT-1, Nrf-2, HO-1 signaling, and TDP 43 accumulation were studied to improve neurobehavioral and neurochemical deficits in MeHg+-treated rodents.

## 5. Limitations

Extensive in vivo knock-in and knock-out studies targeting the SIRT-1, Nrf-2, and HO-1 genes are imperative to elucidate the molecular mechanisms through which Methylmercury (MeHg+) influences Amyotrophic Lateral Sclerosis (ALS) regulation. To corroborate these findings, qualitative assays, such as Western blot analysis, should be employed to verify and elucidate the molecular pathways mediated by SIRT-1, Nrf-2, and HO-1 further. In addition, computational modeling techniques were utilized to predict the interactions of Icariin with the SIRT-1, Nrf-2, and HO-1 receptors at the molecular level. This study observed conformational changes in the three-dimensional structures of these receptors upon binding with Icariin, suggesting a dynamic receptor-ligand interaction. These structural modifications upon Icariin binding are hypothesized to play a role in activating the SIRT-1, Nrf-2, and HO-1 receptors. However, it is important to note a limitation of this study: the absence of mechanistic investigations for in silico validation of these findings."

## 6. Conclusion

Our study demonstrates that icariin exhibits interactions with the signaling pathways of SIRT-1, Nrf-2, HO-1, and TDP-43, influencing pathological manifestations associated with ALS. We observed that icariin mitigates behavioral, biochemical, neurochemical, and gross morphological changes characteristic of an ALS-like phenotype in adult Wistar rats subjected to MeHg+ exposure. This suggests icariin's potential as an effective therapeutic nutraceutical for ALS. Furthermore, our research has identified novel potential biomarkers for ALS in blood plasma, brain homogenates, and CSF. Histological analysis and LFB staining indicate that MeHg+ acts as a neurotoxin, causing damage to neuroglial cells. However, oral administration of icariin at dosages of 15 mg/kg and 30 mg/kg appears to counteract this neurotoxicity, evidenced by regeneration of neuronal populations and promotion of remyelination. To assess the therapeutic efficacy of icariin, we utilized Sirtinol (10 mg/kg) as a comparative agent, which negates icariin's effects by reducing the levels of SIRT-1, Nrf-2, HO-1, and TDP-43. Interestingly, combined treatment with Icariin (30 mg/kg) and Sirtinol (10 mg/kg) demonstrated reversing MeHg+-induced neurotoxicity."

## Ethical approval

The study was carried out in accordance with the Institutional Animal Ethics Committee (IAEC) norms, with registration number 816/PO/ReBiBt/S/04/CPCSEA as protocol no. 26 ISFCP/IAEC/CCSEA/Meeting No:02/2022/Protocol No. 26 approved by the RAB Committee, ISFCP, Moga, Punjab, India.

## Data availability statement

All data generated or analyzed during this study are included in this article. There are no separate or additional files.

## Funding

This work was supported by DST-SERB, Govt. of India (Grant Number: CRG/2021/001009).

## Consent to publish

Authors approve for submitting the publication.

## Consent to participate

Not applicable.

## CRediT authorship contribution statement

**Sarthak Sharma:** Writing – original draft, Project administration, Investigation. **Sidharth Mehan:** Writing – review & editing, Visualization, Validation, Supervision, Investigation, Data curation, Conceptualization. **Zuber Khan:** Writing – review & editing, Software, Formal analysis, Data curation. **Ghanshyam Das Gupta:** Project administration, Funding acquisition, Formal analysis, Data curation. **Acharan S. Narula:** Resources, Funding acquisition, Formal analysis, Conceptualization.

## Declaration of competing interest

The authors declare that they have no known competing financial interests or personal relationships that could have appeared to influence the work reported in this paper.

## Acknowledgments

The authors are grateful to Mr. Parveen Garg, Chairman, ISF College of Pharmacy, Moga (Punjab), India, for their outstanding vision and support. The authors are also grateful to ISF Analytical Laboratory (ISFAL), a NABL- and CDSCO-approved laboratory, for successfully completing all chemical analyses. The authors are also thankful to the Drug Discovery and Development Centre at RTI International in North Carolina, United States, for supplying the Protocol drugs are necessary to carry out the experimental protocol schedule.

## Abbreviations

| | |
|---|---|
| Ach | Acetylcholine |
| AchE | Acetylcholinesterase |
| ALS | Amyotrophic lateral sclerosis |
| ANOVA | Analysis of variance |
| Bax | Bcl-2 associated X protein |
| Bcl-2 | B cell lymphoma-2 |
| BDNF | Brain-derived growth factor |
| cAMP | Cyclic AMP |
| Caspase-3 | Cysteine-aspartic proteases, cysteine aspartases or cysteine-dependent aspartate-directed proteases-3 |
| CAT: | Catalase |
| CNS | Central nervous system |
| CSF | Cerebrospinal fluid |
| ELT | Escape latency time |
| FST | Forced swim test |
| GABA | Gamma amino butyric acid |
| HO-1 | Heme- Oxegenase 1 |
| IL-1β | Interleukin-1Beta |
| LFB | Luxol Fast Blue |
| MBP | Myelin basic protein |
| MeHg | Methylmercury |
| MND | Motor neuron disease |
| MWM | Morris water maze |
| NEFL: | Neurofilament |
| Nrf-2 | Nuclear Factor- Erythroid 2–related factor 2 |
| ODC | Oligodendrocytes |
| OPC: | Oligodendrocyte Precursor Cells |
| SIRT-1 | Silent information regulator 1 |
| TNF-α | Tumor necrosis factor-alpha |
| TSTQ | Time spent in target quadrant |
| TDP-43 | Tar DNA Binding Protein- 43 |
| 5-HT | Serotonin |

## References

[1] E. Minj, S. Upadhayay, S. Mehan, Nrf-2/HO-1 signaling activator acetyl-11-keto-beta boswellic acid (AKBA)-Mediated neuroprotection in methyl mercury-induced experimental model of ALS, Neurochem. Res. 46 (11) (2021) 2867–2884, https://doi.org/10.1007/s11064-021-03366-2.

[2] A. Weerasekera, R. Peeters, D. Sima, T. Dresselaers, S. Sunaert, J. De Vocht, K. Claeys, S. Van Huffel, P. Van Damme, U. Himmelreich, Motor cortex metabolite alterations in amyotrophic lateral sclerosis assessed in vivo using edited and non-edited magnetic resonance spectroscopy, Brain Res. 1718 (2019) 22–31, https://doi.org/10.1016/j.brainres.2019.04.018.

[3] M. Jo, S. Lee, Y.M. Jeon, S. Kim, Y. Kwon, H.J. Kim, The role of TDP-43 propagation in neurodegenerative diseases: integrating insights from clinical and experimental studies, Exp. Mol. Med. 52 (10) (2020) 1652–1662, https://doi.org/10.1038/s12276-020-00513-7.

[4] M.M. Alam, E. Minj, R.K. Yadav, S. Mehan, Neuroprotective potential of adenyl cyclase/cAMP/CREB and mitochondrial CoQ10 activator in amyotrophic lateral sclerosis rats, Curr. Bioact. Compd. 16 (2020).

[5] A. Shandilya, S. Mehan, S. Kumar, P. Sethi, A.S. Narula, A. Alshammari, M. Alharbi, A.F. Alasmari, Activation of IGF-1/GLP-1 signalling via 4-hydroxyiso-leucine prevents motor neuron impairments in experimental ALS-rats exposed to methylmercury-induced neurotoxicity, Molecules 27 (12) (2022) 3878, https://doi.org/10.3390/molecules27123878.

[6] A. Verma, K. Aggarwal, R. Agrawal, K. Pradhan, A. Goyal, Molecular mechanisms regulating the pharmacological actions of icariin with special focus on PI3K-AKT and Nrf-2 signaling pathways, Mol. Biol. Rep. 49 (9) (2022) 9023–9032, https://doi.org/10.1007/s11033-022-07778-3.

[7] C. He, Z. Wang, J. Shi, Pharmacological effects of icariin, Adv. Pharmacol. 87 (2020) 179–203, https://doi.org/10.1016/bs.apha.2019.10.004.

[8] R.K. Yadav, S. Mehan, R. Sahu, S. Kumar, A. Khan, H.A. Makeen, M. Al Bratty, Protective effects of apigenin on methylmercury-induced behavioral/neurochemical abnormalities and neurotoxicity in rats, Hum. Exp. Toxicol. 41 (2022) 9603271221084276, https://doi.org/10.1177/09603271221084276.

[9] R. Sahu, S. Mehan, S. Kumar, A. Prajapati, A. Alshammari, M. Alharbi, M.A. Assiri, A.S. Narula, Effect of alpha-mangostin in the prevention of behavioural and neurochemical defects in methylmercury-induced neurotoxicity in experimental rats, Toxicol Rep 9 (2022) 977–998, https://doi.org/10.1016/j.toxrep.2022.04.023.

[10] A.Z. Herskovits, T.A. Hunter, N. Maxwell, K. Pereira, C.A. Whittaker, G. Valdez, L.P. Guarente, SIRT-1 deacetylase in aging-induced neuromuscular degeneration and amyotrophic lateral sclerosis, Aging Cell 17 (6) (2018) e12839, https://doi.org/10.1111/acel.12839.

[11] B. Rajkhowa, S. Mehan, P. Sethi, A. Prajapati, Activation of SIRT-1 signalling in the prevention of bipolar disorder and related neurocomplications: target activators and influences on neurological dysfunctions, Neurotox. Res. 40 (2) (2022) 670–686, https://doi.org/10.1007/s12640-022-00480-z.

[12] Z. Khan, G.D. Gupta, S. Mehan, Cellular and molecular evidence of multiple sclerosis diagnosis and treatment challenges, J. Clin. Med. 12 (13) (2023) 4274.

[13] I.M. Abd El-Fatah, H.M.A. Abdelrazek, S.M. Ibrahim, D.M. Abdallah, H.S. El-Abhar, Dimethyl fumarate abridged tauo-/amyloidopathy in a D-Galactose/ovariectomy-induced Alzheimer's-like disease: modulation of AMPK/SIRT-1, AKT/CREB/BDNF, AKT/GSK-3β, adiponectin/Adipo1R, and NF-κB/IL-1β/ROS trajectories, Neurochem. Int. 148 (2021) 105082, https://doi.org/10.1016/j.neuint.2021.105082.

[14] W.F. Chen, L. Wu, Z.R. Du, L. Chen, A.L. Xu, X.H. Chen, J.J. Teng, M.S. Wong, Neuroprotective properties of icariin in MPTP-induced mouse model of Parkinson's disease: involvement of PI3K/Akt and MEK/ERK signaling pathways, Phytomedicine : international journal of phytotherapy and phytopharmacology 25 (2017) 93–99, https://doi.org/10.1016/j.phymed.2016.12.017.

[15] H.T. Hsu, Y.L. Yang, W.H. Chang, W.Y. Fang, S.H. Huang, S.H. Chou, Y.C. Lo, Hyperbaric oxygen therapy improves Parkinson's disease by promoting mitochondrial biogenesis via the SIRT-1/PGC-1α pathway, Biomolecules 12 (5) (2022) 661, https://doi.org/10.3390/biom12050661.

[16] N. Sharma, A. Shandilya, N. Kumar, S. Mehan, Dysregulation of SIRT-1 signaling in multiple sclerosis and neuroimmune disorders: a systematic review of sirtuin activators as potential immunomodulators and their influences on other dysfunctions, Endocr. Metab. Immune Disord. - Drug Targets 21 (10) (2021) 1845–1868, https://doi.org/10.2174/1871530321666210309112234.

[17] S. Chhabra, S. Mehan, Z. Khan, G.D. Gupta, A.S. Narula, Matrine mediated neuroprotective potential in experimental multiple sclerosis: evidence from CSF, blood markers, brain samples and in-silico investigations, J. Neuroimmunol. 384 (2023) 578200, https://doi.org/10.1016/j.jneuroim.2023.578200. Advance online publication.

[18] B. Shal, A. Khan, A. Ullah Khan, R. Ullah, M. Naveed, G. Ali, S. Ul Islam, I. Ul Haq, B. Mirza, S. Khan, Coagulansin-A improves spatial memory in 5xFAD Tg mice by targeting Nrf-2/NF-κB and Bcl-2 pathway, Int. Immunopharm. 109 (2022) 108860, https://doi.org/10.1016/j.intimp.2022.108860.

[19] A. Ali, S.A. Shah, N. Zaman, M.N. Uddin, W. Khan, A. Ali, M. Riaz, A. Kamil, Vitamin D exerts neuroprotection via SIRT-1/nrf-2/NF-kB signaling pathways against D-galactose-induced memory impairment in adult mice, Neurochem. Int. 142 (2021) 104893, https://doi.org/10.1016/j.neuint.2020.104893.

[20] M. Abdalkader, R. Lampinen, K.M. Kanninen, T.M. Malm, J.R. Liddell, Targeting nrf-2 to suppress ferroptosis and mitochondrial dysfunction in neurodegeneration, Front. Neurosci. 12 (2018) 466, https://doi.org/10.3389/fnins.2018.00466.

[21] Y. Wang, L. Gao, J. Chen, Q. Li, L. Huo, Y. Wang, H. Wang, J. Du, Pharmacological modulation of nrf-2/HO-1 signaling pathway as a therapeutic target of Parkinson's disease, Front. Pharmacol. 12 (2021) 757161, https://doi.org/10.3389/fphar.2021.757161.

[22] R.B. Mythri, C. Venkateshappa, G. Harish, A. Mahadevan, U.B. Muthane, T.C. Yasha, M.M. Srinivas Bharath, S.K. Shankar, Evaluation of markers of oxidative stress, antioxidant function and astrocytic proliferation in the striatum and frontal cortex of Parkinson's disease brains, Neurochem. Res. 36 (8) (2011) 1452–1463, https://doi.org/10.1007/s11064-011-0471-9.

[23] C. Li, R. Wang, C. Hu, H. Wang, Q. Ma, S. Chen, Y. He, Pyridoxine exerts antioxidant effects in cell model of Alzheimer's disease via the Nrf-2/HO-1 pathway, Cell. Mol. Biol. 64 (10) (2018) 119–124.

[24] S. Upadhayay, S. Mehan, A. Prajapati, P. Sethi, M. Suri, A. Zawawi, M.N. Almashjary, S. Tabrez, Nrf-2/HO-1 signaling stimulation through acetyl-11-keto-beta-boswellic acid (AKBA) provides neuroprotection in ethidium bromide-induced experimental model of multiple sclerosis, Genes 13 (8) (2022) 1324, https://doi.org/10.3390/genes13081324.

[25] B.I. Arioz, B. Tastan, E. Tarakcioglu, K.U. Tufekci, M. Olcum, N. Ersoy, A. Bagriyanik, K. Genc, S. Genc, Melatonin attenuates LPS-induced acute depressive-like behaviors and microglial NLRP3 inflammasome activation through the SIRT-1/nrf-2 pathway, Front. Immunol. 10 (2019) 1511, https://doi.org/10.3389/fimmu.2019.01511.

[26] J.M. Rosa, F.L. Pazini, M.P. Cunha, A.R.S. Colla, L.M. Manosso, G. Mancini, A.C.G. Souza, A.F. de Bem, R.D. Prediger, A.L.S. Rodrigues, Antidepressant effects of creatine on amyloid $\beta_{1-40}$-treated mice: the role of GSK-3β/Nrf-2 pathway, Progress in neuro-psychopharmacology & biological psychiatry 86 (2018) 270–278, https://doi.org/10.1016/j.pnpbp.2018.05.001.

[27] N. Mori, A. Yasutake, M. Marumoto, K. Hirayama, Methylmercury inhibits electron transport chain activity and induces cytochrome c release in cerebellum mitochondria, J. Toxicol. Sci. 36 (3) (2011) 253–259, https://doi.org/10.2131/jts.36.253.

[28] X. Gao, D. He, D. Liu, G. Hu, Y. Zhang, T. Meng, Y. Su, A. Zhou, B. Huang, J. Du, S. Fu, Beta-naphthoflavone inhibits LPS-induced inflammation in BV-2 cells via AKT/Nrf-2/HO-1-NF-κB signaling axis, Immunobiology 225 (4) (2020) 151965, https://doi.org/10.1016/j.imbio.2020.151965.

[29] A. Patruno, E. Costantini, A. Ferrone, M. Pesce, F. Diomede, O. Trubiani, M. Reale, Short ELF-EMF exposure targets SIRT-1/nrf-2/HO-1 signaling in THP-1 cells, Int. J. Mol. Sci. 21 (19) (2020) 7284, https://doi.org/10.3390/ijms21197284.

[30] D. Yang, X. Tan, Z. Lv, B. Liu, R. Baiyun, J. Lu, Z. Zhang, Regulation of SIRT-1/Nrf-2/TNF-α signaling pathway by luteolin is critical to attenuate acute mercuric chloride exposure induced hepatotoxicity, Sci. Rep. 6 (2016) 37157, https://doi.org/10.1038/srep37157.

[31] S. Mehan, Editorial: therapeutic modulators inhibiting neuromuscular and motor neuron degeneration, Front. Neurosci. 17 (2023) 1188945, https://doi.org/10.3389/fnins.2023.1188945.

[32] L.R. Li, G. Sethi, X. Zhang, C.L. Liu, Y. Huang, Q. Liu, B.X. Ren, F.R. Tang, The neuroprotective effects of icariin on ageing, various neurological, neuropsychiatric disorders, and brain injury induced by radiation exposure, Aging 14 (3) (2022) 1562–1588, https://doi.org/10.18632/aging.203893.

[33] T.I. Adelusi, A.Q.K. Oyedele, I.D. Boyenle, A.T. Ogunlana, R.O. Adeyemi, C.D. Ukachi, M.O. Idris, O.T. Olaoba, I.O. Adedotun, O.E. Kolawole, Y. Xiaoxing, M. Abdul-Hammed, Molecular modeling in drug discovery, Inform. Med. Unlocked 29 (2022) 100880.

[34] H. Yu, J. Shi, Y. Lin, Y. Zhang, Q. Luo, S. Huang, S. Wang, J. Wei, J. Huang, C. Li, L. Ji, Icariin ameliorates Alzheimer's disease pathology by alleviating myelin injury in 3 × tg-AD mice, Neurochem. Res. 47 (4) (2022) 1049–1059, https://doi.org/10.1007/s11064-021-03507-7.

[35] A. Prajapati, S. Mehan, Z. Khan, The role of Smo-Shh/Gli signaling activation in the prevention of neurological and ageing disorders, Biogerontology 24 (4) (2023) 493–531, https://doi.org/10.1007/s10522-023-10034-1.

[36] B. Pan, L. Xu, J. Weng, Y. Wang, H. Ji, B. Han, X. Zhu, Y. Liu, Effects of icariin on alleviating schizophrenia-like symptoms by regulating the miR-144-3p/ATP1B2/mTOR signalling pathway, Neurosci. Lett. 791 (2022) 136918, https://doi.org/10.1016/j.neulet.2022.136918.

[37] C.T. Wu, M.C. Chen, S.H. Liu, T.H. Yang, L.H. Long, S.S. Guan, C.M. Chen, Bioactive flavonoids icaritin and icariin protect against cerebral ischemia-reperfusion-associated apoptosis and extracellular matrix accumulation in an ischemic stroke mouse model, Biomedicines 9 (11) (2021) 1719, https://doi.org/10.3390/biomedicines9111719.

[38] H.R. Zhu, Z.Y. Wang, X.L. Zhu, X.X. Wu, E.G. Li, Y. Xu, Icariin protects against brain injury by enhancing SIRT-1-dependent PGC-1 alpha expression in experimental stroke, Neuropharmacology 59 (1–2) (2010) 70–76, https://doi.org/10.1016/j.neuropharm.2010.03.017.

[39] T. Ali, T. Kim, S.U. Rehman, M.S. Khan, F.U. Amin, M. Khan, M. Ikram, M.O. Kim, Natural dietary supplementation of anthocyanins via PI3K/Akt/Nrf-2/HO-1 pathways mitigate oxidative stress, neurodegeneration, and memory impairment in a mouse model of Alzheimer's disease, Mol. Neurobiol. 55 (7) (2018) 6076–6093, https://doi.org/10.1007/s12035-017-0798-6.

[40] S. Mehan, S. Parveen, S. Kalra, Adenyl cyclase activator forskolin protects against Huntington's disease-like neurodegenerative disorders, Neural regeneration research 12 (2) (2017) 290–300, https://doi.org/10.4103/1673-5374.200812.

[41] C. Huang, J. Wu, D. Chen, J. Jin, Y. Wu, Z. Chen, Effects of sulforaphane in the central nervous system, Eur. J. Pharmacol. 853 (2019) 153–168, https://doi.org/10.1016/j.ejphar.2019.03.010.

[42] E. Minj, R.K. Yadav, S. Mehan, Targeting abnormal nrf-2/HO-1 signaling in amyotrophic lateral sclerosis: current insights on drug targets and influences on neurological disorders, Curr. Mol. Med. 21 (8) (2021) 630–644, https://doi.org/10.2174/1566524021666210111104920.

[43] I. Buendia, P. Michalska, E. Navarro, I. Gameiro, J. Egea, R. León, Nrf-2-ARE pathway: an emerging target against oxidative stress and neuroinflammation in neurodegenerative diseases, Pharmacol. Ther. 157 (2016) 84–104, https://doi.org/10.1016/j.pharmthera.2015.11.003.

[44] H. Kaur, A. Kumar, A.S. Jaggi, N. Singh, Pharmacologic investigations on the role of Sirt-1 in neuroprotective mechanism of postconditioning in mice, J. Surg. Res. 197 (1) (2015) 191–200, https://doi.org/10.1016/j.jss.2015.03.010.

[45] N. Kumar, N. Sharma, R. Khera, R. Gupta, S. Mehan, Guggulsterone ameliorates ethidium bromide-induced experimental model of multiple sclerosis via restoration of behavioral, molecular, neurochemical and morphological alterations in rat brain, Metab. Brain Dis. 36 (5) (2021) 911–925, https://doi.org/10.1007/s11011-021-00691-x.

[46] R. Gupta, S. Mehan, P. Sethi, A. Prajapati, A. Alshammari, M. Alharbi, H.A. Al-Mazroua, A.S. Narula, Smo-shh agonist purmorphamine prevents neurobehavioral and neurochemical defects in 8-OH-DPAT-induced experimental model of obsessive-compulsive disorder, Brain Sci. 12 (3) (2022) 342, https://doi.org/10.3390/brainsci12030342.

[47] P. Duggal, K.S. Jadaun, E.M. Siqqiqui, S. Mehan, Investigation of low dose cabazitaxel potential as microtubule stabilizer in experimental model of Alzheimer's disease: restoring neuronal cytoskeleton, Curr. Alzheimer Res. 17 (7) (2020) 601–615, https://doi.org/10.2174/1567205017666201007120112.

[48] K. Rajdev, E.M. Siddiqui, K.S. Jadaun, S. Mehan, Neuroprotective potential of solanesol in a combined model of intracerebral and intraventricular hemorrhage in rats, IBRO reports 8 (2020) 101–114, https://doi.org/10.1016/j.ibror.2020.03.001.

[49] A. Sharma, S. Bhalla, S. Mehan, PI3K/AKT/mTOR signalling inhibitor chrysophanol ameliorates neurobehavioural and neurochemical defects in propionic acid-induced experimental model of autism in adult rats, Metab. Brain Dis. 37 (6) (2022) 1909–1929, https://doi.org/10.1007/s11011-022-01026-0.

[50] S. Mehan, S. Bhalla, E.M. Siddiqui, N. Sharma, A. Shandilya, A. Khan, Potential roles of glucagon-like peptide-1 and its analogues in dementia targeting impaired insulin secretion and neurodegeneration, Degener. Neurol. Neuromuscul. Dis. 12 (2022) 31–59, https://doi.org/10.2147/DNND.S247153.

[51] A. Tiwari, R. Khera, S. Rahi, S. Mehan, H.A. Makeen, Y.H. Khormi, M.U. Rehman, A. Khan, Neuroprotective effect of α-mangostin in the ameliorating propionic acid-induced experimental model of autism in wistar rats, Brain Sci. 11 (3) (2021) 288, https://doi.org/10.3390/brainsci11030288.

[52] R. Sharma, S. Rahi, S. Mehan, Neuroprotective potential of solanesol in intracerebroventricular propionic acid induced experimental model of autism: insights from behavioral and biochemical evidence, Toxicol Rep 6 (2019) 1164–1175, https://doi.org/10.1016/j.toxrep.2019.10.019.

[53] A. Yasutake, M. Nagano, A. Nakano, Simple method for methylmercury estimation in biological samples using atomic absorption spectroscopy, J. Health Sci. 51 (2) (2005) 220–223.

[54] C. Gnanaraj, M. Sekar, S. Fuloria, S.S. Swain, S.H. Gan, K. Chidambaram, N.N.I.M. Rani, T. Balan, S. Stephenie, P.T. Lum, S. Jeyabalan, M.Y. Begum, V. Chandramohan, L. Thangavelu, V. Subramaniyan, N.K. Fuloria, Silico molecular docking analysis of karanjin against Alzheimer's and Parkinson's diseases as a potential natural lead molecule for new drug design, development and therapy, Molecules 27 (9) (2022) 2834, https://doi.org/10.3390/molecules27092834.

[55] S. Kumar, F. Abbas, I. Ali, M.K. Gupta, S. Kumar, M. Garg, D. Kumar, Integrated network pharmacology and in-silico approaches to decipher the pharmacological mechanism of Selaginella tamariscina in the treatment of non-small cell lung cancer, Phytomedicine 3 (2) (2023) 100419.

[56] A. Giri, S. Mehan, Z. Khan, G.D. Gupta, A.S. Narula, Melatonin-mediated IGF-1/GLP-1 activation in experimental OCD rats: evidence from CSF, blood plasma, brain and in-silico investigations, Biochem. Pharmacol. 217 (2023) 115831, https://doi.org/10.1016/j.bcp.2023.115831. Advance online publication.

[57] M.N. Rahman, J.Z. Vlahakis, D. Vukomanovic, W.A. Szarek, K. Nakatsu, Z. Jia, X-ray crystal structure of human heme oxygenase-1 with (2R,4S)-2-[2-(4-chlorophenyl)ethyl]-2-[(1H-imidazole-1-yl)methyl]-4[((5-trifluoromethylpyridin-2- yl)thio)methyl]-1,3-dioxolane: a novel, inducible binding mode, J. Med. Chem. 52 (15) (2009) 4946–4950.

[58] D. Cao, M. Wang, X. Qiu, D. Liu, H. Jiang, N. Yang, R.M. Xu, Structural basis for allosteric, substrate-dependent stimulation of SIRT-1 activity by resveratrol, Gene Dev. 29 (12) (2015) 1316–1325.

[59] S. Cosconati, S. Forli, A.L. Perryman, R. Harris, D.S. Goodsell, A.J. Olson, Virtual screening with AutoDock: theory and practice 5 (6) (2010) 597–607.

[60] G.M. Morris, H. Ruth, W. Lindstrom, M.F. Sanner, R.K. Belew, D.S. Goodsell, A.J. Olson, AutoDock 4 and AutoDockTools 4: automated docking with selective receptor flexibility, J. Comput. Chem. 30 (16) (2009) 2785–2791.

[61] N.M. O'Boyle, M. Banck, C.A. James, C. Morley, T. Vandermeersch, G.R. Hutchison, Open babel: an open chemical toolbox, J. Cheminf. 3 (10) (2011) 1–14.

[62] S. Dallakyan, A.J. Olson, Small-molecule library screening by docking with PyRx, Methods Mol. Biol. 1263 (2015) 243–250.

[63] S. Kumar, S. Sengupta, I. Ali, M.K. Gupta, H. Lalhlenmawia, S. Azizov, D. Kumar, Identification and exploration of quinazoline-1,2,3-triazole inhibitors targeting EGFR in lung cancer, J. Biomol. Struct. Dyn. 1–20 (2023).

[64] A. Lorente Pons, A. Higginbottom, J. Cooper-Knock, A. Alrafiah, E. Alofi, J. Kirby, P.J. Shaw, J.D. Wood, J.R. Highley, Oligodendrocyte pathology exceeds axonal pathology in white matter in human amyotrophic lateral sclerosis, J. Pathol. 251 (3) (2020) 262–271, https://doi.org/10.1002/path.5455.

[65] A. Chiò, M. Pagani, F. Agosta, A. Calvo, A. Cistaro, M. Filippi, Neuroimaging in amyotrophic lateral sclerosis: insights into structural and functional changes, Lancet Neurol. 13 (12) (2014) 1228–1240, https://doi.org/10.1016/S1474-4422(14)70167-X.

[66] E. Traiffort, S. Morisset-Lopez, M. Moussaed, A. Zahaf, Defective oligodendroglial lineage and demyelination in amyotrophic lateral sclerosis, Int. J. Mol. Sci. 22 (7) (2021) 3426, https://doi.org/10.3390/ijms22073426.

[67] Y. Liu, H. Li, X. Wang, J. Huang, D. Zhao, Y. Tan, Z. Zhang, Z. Zhang, L. Zhu, B. Wu, Z. Chen, W. Peng, Anti-Alzheimers molecular mechanism of icariin: insights from gut microbiota, metabolomics, and network pharmacology, J. Transl. Med. 21 (1) (2023) 277, https://doi.org/10.1186/s12967-023-04137-z.

[68] P. Sethi, S. Mehan, Z. Khan, S. Chhabra, Acetyl-11-keto-beta boswellic acid(AKBA) modulates CSTC-pathway by activating SIRT-1/Nrf-2-HO-1 signalling in experimental rat model of obsessive-compulsive disorder: evidenced by CSF, blood plasma and histopathological alterations, Neurotoxicology 98 (2023) 61–85, https://doi.org/10.1016/j.neuro.2023.08.001.

[69] J. Wu, J.Q. Qu, Y.J. Zhou, Y.J. Zhou, Y.Y. Li, N.Q. Huang, C.M. Deng, Y. Luo, Icariin improves cognitive deficits by reducing the deposition of β-amyloid peptide and inhibition of neurons apoptosis in SAMP8 mice, Neuroreport 31 (9) (2020) 663–671, https://doi.org/10.1097/WNR.0000000000001466.

[70] A.B. Niculescu, H. Le-Niculescu, K. Roseberry, S. Wang, J. Hart, A. Kaur, H. Robertson, T. Jones, A. Strasburger, A. Williams, S.M. Kurian, B. Lamb, A. Shekhar, D.K. Lahiri, A.J. Saykin, Blood biomarkers for memory: toward early detection of risk for Alzheimer disease, pharmacogenomics, and repurposed drugs, Mol. Psychiatr. 25 (8) (2020) 1651–1672, https://doi.org/10.1038/s41380-019-0602-2.

[71] W.T. Yang, X.W. Zheng, S. Chen, C.S. Shan, Q.Q. Xu, J.Z. Zhu, X.Y. Bao, Y. Lin, G.Q. Zheng, Y. Wang, Chinese herbal medicine for Alzheimer's disease: clinical evidence and possible mechanism of neurogenesis, Biochem. Pharmacol. 141 (2017) 143–155, https://doi.org/10.1016/j.bcp.2017.07.002.

[72] H. Xiao, N. Wignall, E.S. Brown, An open-label pilot study of icariin for co-morbid bipolar and alcohol use disorder, Am. J. Drug Alcohol Abuse 42 (2) (2016) 162–167, https://doi.org/10.3109/00952990.2015.1114118.

[73] J.F. Zhang, Y.L. Zhang, Y.C. Wu, The role of SIRT-1 in ischemic stroke: pathogenesis and therapeutic strategies, Front. Neurosci. 12 (2018) 833, https://doi.org/10.3389/fnins.2018.00833.

[74] Y. Zhang, L. Yin, N. Zheng, L. Zhang, J. Liu, W. Liang, Q. Wang, Icariin enhances remyelination process after acute demyelination induced by cuprizone exposure, Brain Res. Bull. 130 (2017) 180–187, https://doi.org/10.1016/j.brainresbull.2017.01.025.

[75] R. Zeng, X. Wang, Q. Zhou, X. Fu, Q. Wu, Y. Lu, J. Shi, J.E. Klaunig, S. Zhou, Icariin protects rotenone-induced neurotoxicity through induction of SIRT3, Toxicol. Appl. Pharmacol. 379 (2019) 114639, https://doi.org/10.1016/j.taap.2019.114639.

[76] H. Joo, J. Bae, J.S. Lee, Y. Bang, B.J. Lee, J.W. Park, K. Lee, J.H. Cho, Y. Bu, Icariin improves functional behavior in a mouse model of traumatic brain injury and promotes synaptic plasticity markers, Planta Med. 85 (3) (2019) 231–238, https://doi.org/10.1055/a-0753-0400.

[77] P. Mishra, A.K. Mittal, H. Kalonia, S. Madan, S. Ghosh, J.K. Sinha, S.K. Rajput, SIRT-1 promotes neuronal fortification in neurodegenerative diseases through attenuation of pathological hallmarks and enhancement of cellular lifespan, Curr. Neuropharmacol. 19 (7) (2021) 1019–1037, https://doi.org/10.2174/1570159X18666200729111744.

[78] M. Wiciński, J. Erdmann, A. Nowacka, O. Kuźmiński, K. Michalak, K. Janowski, J. Ohla, A. Biernaciak, M. Szambelan, J. Zabrzyński, Natural phytochemicals as SIRT activators-focus on potential biochemical mechanisms, Nutrients 15 (16) (2023) 3578, https://doi.org/10.3390/nu15163578.

[79] X. He, J. Sun, X. Huang, Expression of caspase-3, Bax and Bcl-2 in hippocampus of rats with diabetes and subarachnoid hemorrhage, Exp. Ther. Med. 15 (1) (2018) 873–877, https://doi.org/10.3892/etm.2017.5438.

[80] K.J. Speaker, S.S. Cox, M.M. Paton, A. Serebrakian, T. Maslanik, B.N. Greenwood, M. Fleshner, Six weeks of voluntary wheel running modulates inflammatory protein (MCP-1, IL-6, and IL-10) and DAMP (Hsp 72) responses to acute stress in white adipose tissue of lean rats, Brain Behav. Immun. 39 (2014) 87–98, https://doi.org/10.1016/j.bbi.2013.10.028.

[81] J.E. Pierce, J. Péron, The basal ganglia and the cerebellum in human emotion, Soc. Cognit. Affect Neurosci. 15 (5) (2020) 599–613, https://doi.org/10.1093/scan/nsaa076.

[82] H.J. Lee, A.J. Weitz, D. Bernal-Casas, B.A. Duffy, M. Choy, A.V. Kravitz, A.C. Kreitzer, J.H. Lee, Activation of direct and indirect pathway medium spiny neurons drives distinct brain-wide responses, Neuron 91 (2) (2016) 412–424, https://doi.org/10.1016/j.neuron.2016.06.010.

[83] S. Peters, K. Broberg, V. Gallo, M. Levi, M. Kippler, P. Vineis, J. Veldink, L. van den Berg, L. Middleton, R.C. Travis, M.M. Bergmann, D. Palli, S. Grioni, R. Tumino, A. Elbaz, T. Vlaar, F. Mancini, T. Kühn, V. Katzke, A. Agudo, R. Vermeulen, Blood metal levels and amyotrophic lateral sclerosis risk: a prospective cohort, Ann. Neurol. 89 (1) (2021) 125–133, https://doi.org/10.1002/ana.25932.

[84] R. Oggiano, A. Pisano, A. Sabalic, C. Farace, G. Fenu, S. Lintas, G. Forte, B. Bocca, R. Madeddu, An overview on amyotrophic lateral sclerosis and cadmium, Neurol. Sci. : official journal of the Italian Neurological Society and of the Italian Society of Clinical Neurophysiology 42 (2) (2021) 531–537, https://doi.org/10.1007/s10072-020-04957-7.

[85] B.R. Foerster, M.G. Pomper, B.C. Callaghan, M. Petrou, R.A. Edden, M.A. Mohamed, R.C. Welsh, R.C. Carlos, P.B. Barker, E.L. Feldman, An imbalance between excitatory and inhibitory neurotransmitters in amyotrophic lateral sclerosis revealed by use of 3-T proton magnetic resonance spectroscopy, JAMA Neurol. 70 (8) (2013) 1009–1016, https://doi.org/10.1001/jamaneurol.2013.234.

[86] N. Shahsavani, H. Kataria, S. Karimi-Abdolrezaee, Mechanisms and repair strategies for white matter degeneration in CNS injury and diseases, Biochimica et biophysica acta. Molecular basis of disease 1867 (6) (2021) 166117, https://doi.org/10.1016/j.bbadis.2021.166117.

[87] H. Blasco, S. Mavel, P. Corcia, P.H. Gordon, The glutamate hypothesis in ALS: pathophysiology and drug development, Curr. Med. Chem. 21 (31) (2014) 3551–3575, https://doi.org/10.2174/0929867321666140916120118.

[88] C.L. Lin, Q. Kong, G.D. Cuny, M.A. Glicksman, Glutamate transporter EAAT2: a new target for the treatment of neurodegenerative diseases, Future Med. Chem. 4 (13) (2012) 1689–1700, https://doi.org/10.4155/fmc.12.122.

[89] E. Martin, W. Cazenave, A.E. Allain, D. Cattaert, P. Branchereau, Implication of 5-HT in the dysregulation of chloride homeostasis in prenatal spinal motoneurons from the G93A mouse model of amyotrophic lateral sclerosis, Int. J. Mol. Sci. 21 (3) (2020) 1107, https://doi.org/10.3390/ijms21031107.

[90] H. El Oussini, J. Scekic-Zahirovic, P. Vercruysse, C. Marques, S. Dirrig-Grosch, S. Dieterlé, G. Picchiarelli, J. Sinniger, C. Rouaux, L. Dupuis, Degeneration of serotonin neurons triggers spasticity in amyotrophic lateral sclerosis, Ann. Neurol. 82 (3) (2017) 444–456, https://doi.org/10.1002/ana.25030.

[91] D. Kulick, E. Moon, R.M. Riffe, G. Teicher, S. Van Deursen, A. Berson, W. He, G. Aaron, G.B. Downes, S. Devoto, A. O'Neil, Amyotrophic lateral sclerosis-associated persistent organic pollutant *cis*-chlordane causes $GABA_A$-independent toxicity to motor neurons, providing evidence toward an environmental component of sporadic amyotrophic lateral sclerosis, ACS Chem. Neurosci. 13 (24) (2022) 3567–3577, https://doi.org/10.1021/acschemneuro.2c00452.

[92] B.R. Foerster, B.C. Callaghan, M. Petrou, R.A. Edden, T.L. Chenevert, E.L. Feldman, Decreased motor cortex γ-aminobutyric acid in amyotrophic lateral sclerosis, Neurology 78 (20) (2012) 1596–1600, https://doi.org/10.1212/WNL.0b013e3182563b57.

[93] M. Kakkonen, S. Naulaerts, K. Op De Beeck, K. Laukens, G. Van Camp, A.R. Weseler, A. Bast, G.R.M.M. Haenen, G. Haegeman, W. Vanden Berghe, Withaferin A induces heme oxygenase (HO-1) expression in endothelial cells via activation of the Keap1/Nrf-2 pathway, Biochem. Pharmacol. 109 (2016) 48–61.

[94] X. Zuo, J. Zhou, Y. Li, K. Wu, Z. Chen, Z. Luo, X. Zhang, Y. Liang, M.A. Esteban, Y. Zhou, X.D. Fu, TDP-43 aggregation induced by oxidative stress causes global mitochondrial imbalance in ALS, Nat. Struct. Mol. Biol. 28 (2) (2021) 132–142, https://doi.org/10.1038/s41594-020-00537-7.

[95] T. Yamashita, S. Kwak, The molecular link between inefficient GluA2 Q/R site-RNA editing and TDP-43 pathology in motor neurons of sporadic amyotrophic lateral sclerosis patients, Brain Res. 1584 (2014) 28–38, https://doi.org/10.1016/j.brainres.2013.12.011.

[96] V.M. Van Deerlin, J.B. Leverenz, L.M. Bekris, T.D. Bird, W. Yuan, L.B. Elman, D. Clay, E.M. Wood, A.S. Chen-Plotkin, M. Martinez-Lage, E. Steinbart, L. McCluskey, M. Grossman, M. Neumann, I.L. Wu, W.S. Yang, R. Kalb, D.R. Galasko, T.J. Montine, J.Q. Trojanowski, C.E. Yu, TARDBP mutations in amyotrophic lateral sclerosis with TDP-43 neuropathology: a genetic and histopathological analysis, Lancet Neurol. 7 (5) (2008) 409–416, https://doi.org/10.1016/S1474-4422(08)70071-1.

[97] J. Brettschneider, K. Del Tredici, J.B. Toledo, J.L. Robinson, D.J. Irwin, M. Grossman, E. Suh, V.M. Van Deerlin, E.M. Wood, Y. Baek, L. Kwong, E.B. Lee, L. Elman, L. McCluskey, L. Fang, S. Feldengut, A.C. Ludolph, V.M. Lee, H. Braak, J.Q. Trojanowski, Stages of pTDP-43 pathology in amyotrophic lateral sclerosis, Ann. Neurol. 74 (1) (2013) 20–38, https://doi.org/10.1002/ana.23937.

[98] S. Abrahams, L.H. Goldstein, J. Suckling, V. Ng, A. Simmons, X. Chitnis, L. Atkins, S.C. Williams, P.N. Leigh, Frontotemporal white matter changes in amyotrophic lateral sclerosis, J. Neurol. 252 (3) (2005) 321–331, https://doi.org/10.1007/s00415-005-0646-x.

[99] P.S. Mishra, D.K. Dhull, A. Nalini, K. Vijayalakshmi, T.N. Sathyaprabha, P.A. Alladi, T.R. Raju, Astroglia acquires a toxic neuroinflammatory role in response to the cerebrospinal fluid from amyotrophic lateral sclerosis patients, J. Neuroinflammation 13 (1) (2016) 212, https://doi.org/10.1186/s12974-016-0698-0.

[100] M. Iwai-Shimada, T. Takahashi, M.S. Kim, M. Fujimura, H. Ito, T. Toyama, A. Naganuma, G.W. Hwang, Methylmercury induces the expression of TNF-α selectively in the brain of mice, Sci. Rep. 6 (2016) 38294, https://doi.org/10.1038/srep38294.

[101] E. Zucchi, V. Bonetto, G. Sorarù, I. Martinelli, P. Parchi, R. Liguori, J. Mandrioli, Neurofilaments in motor neuron disorders: towards promising diagnostic and prognostic biomarkers, Mol. Neurodegener. 15 (1) (2020) 58, https://doi.org/10.1186/s13024-020-00406-3.

[102] D.W. Li, H. Ren, A. Jeromin, M. Liu, D. Shen, H. Tai, Q. Ding, X. Li, L. Cui, Diagnostic performance of neurofilaments in Chinese patients with amyotrophic lateral sclerosis: a prospective study, Front. Neurol. 9 (2018) 726, https://doi.org/10.3389/fneur.2018.00726.

[103] J. Gaiottino, N. Norgren, R. Dobson, J. Topping, A. Nissim, A. Malaspina, J.P. Bestwick, A.U. Monsch, A. Regeniter, R.L. Lindberg, L. Kappos, D. Leppert, A. Petzold, G. Giovannoni, J. Kuhle, Increased neurofilament light chain blood levels in neurodegenerative neurological diseases, PLoS One 8 (9) (2013) e75091, https://doi.org/10.1371/journal.pone.0075091.

[104] D. Gagliardi, M. Meneri, D. Saccomanno, N. Bresolin, G.P. Comi, S. Corti, Diagnostic and prognostic role of blood and cerebrospinal fluid and blood neurofilaments in amyotrophic lateral sclerosis: a review of the literature, Int. J. Mol. Sci. 20 (17) (2019) 4152, https://doi.org/10.3390/ijms20174152.

[105] R.H. Chipika, G. Mulkerrin, P.F. Pradat, A. Murad, F. Ango, C. Raoul, P. Bede, Cerebellar pathology in motor neuron disease: neuroplasticity and neurodegeneration, Neural regeneration research 17 (11) (2022) 2335–2341, https://doi.org/10.4103/1673-5374.336139.

[106] A. Brunet, G. Stuart-Lopez, T. Burg, J. Scekic-Zahirovic, C. Rouaux, Cortical circuit dysfunction as a potential driver of amyotrophic lateral sclerosis, Front. Neurosci. 14 (2020) 363, https://doi.org/10.3389/fnins.2020.00363.

[107] R.A. Grant, P.S. Sharp, A.J. Kennerley, J. Berwick, A. Grierson, T. Ramesh, T.J. Prescott, Abnormalities in whisking behaviour are associated with lesions in brain stem nuclei in a mouse model of amyotrophic lateral sclerosis, Behav. Brain Res. 259 (2014) 274–283, https://doi.org/10.1016/j.bbr.2013.11.002.

[108] R.K. Yadav, E. Minz, S. Mehan, Understanding abnormal c-JNK/p38MAPK signaling in amyotrophic lateral sclerosis: potential drug targets and influences on neurological disorders, CNS Neurol. Disord. - Drug Targets 20 (5) (2021) 417–429, https://doi.org/10.2174/1871527320666210126113848.